# Ergodic properties of a generic nonintegrable quantum many-body system in the thermodynamic limit

Tomaž Prosen

*Physics Department, Faculty of Mathematics and Physics, University of Ljubljana, Jadranska 19, 1111 Ljubljana, Slovenia*
(Received 18 August 1998; revised manuscript received 29 March 1999)

We study a generic but simple nonintegrable quantum *many-body* system of *locally* interacting particles, namely, a kicked-parameter $(t,V)$ model of spinless fermions on a one-dimensional lattice (equivalent to a kicked Heisenberg *XX-Z* chain of 1/2 spins). The statistical properties of the dynamics (quantum ergodicity and quantum mixing) and the nature of quantum transport in the *thermodynamic limit* are considered as the kick parameters (which control the degree of nonintegrability) are varied. We find and demonstrate *ballistic* transport and nonergodic, nonmixing dynamics (implying infinite conductivity at all temperatures) in the *integrable* regime of zero or very small kick parameters, and more generally and importantly, also in the *nonintegrable* regime of *intermediate* values of kicked parameters, whereas only for sufficiently large kick parameters do we recover quantum ergodicity and mixing implying normal (diffusive) transport. We propose an order parameter (charge stiffness $D$) which controls the phase transition from nonmixing and nonergodic dynamics (ordered phase, $D>0$) to mixing and ergodic dynamics (disordered phase, $D=0$) in the thermodynamic limit. Furthermore, we find *exponential decay of time correlation functions* in the regime of mixing dynamics. The results are obtained consistently within three different numerical and analytical approaches: (i) time evolution of a finite system and direct computation of time correlation functions, (ii) full diagonalization of finite systems and statistical analysis of stationary data, and (iii) algebraic construction of quantum invariants of motion of an infinite system, in particular the time-averaged observables. [S1063-651X(99)10710-3]

PACS number(s): 05.45.−a, 05.30.Fk, 72.10.Bg

## I. INTRODUCTION

It has been a common belief for a long time that a large system of sufficiently many interacting particles should uniformly fill the entire available phase space. This is known as the *ergodic hypothesis*, one of the cornerstones of statistical mechanics, and is a necessary assumption to justify the use of canonical ensembles and a derivation of fundamental laws of statistical physics, such as transport laws (e.g., Ohm's law or Fourier's law).

However, the proof of this, together with the precise conditions for the validity of the ergodic hypothesis is still one of the most fundamental unsolved problems of theoretical physics. Even in the context of purely classical dynamics, the ergodic theory [1,2], though it is an involved and beautiful mathematical discipline, can make strong statements only for a very limited class of systems, while generic dynamical systems, especially those consisting of many interacting particles, are far from being understood [3–8]. Even less is known about ergodic properties of generic *quantum* many-body systems, which is precisely the objective of this paper. A closed (finite) and bounded quantum system of size $L$ and with a finite number $N$ of particles has a discrete spectrum, hence its time evolution is quasiperiodic, and accordingly it is nonergodic and nonmixing, as we shall define below. However, in the thermodynamic limit (TL), of diverging size $L\to\infty$ and density of particles $\rho=N/L$ fixed, the spectrum of the quantum propagator may accuire a continuous component, and one may expect genuine properties of quantum ergodicity and quantum mixing to set in provided the strength of the nonlinear interaction is sufficiently strong. In this paper we deal with general nonautonomous many-body

systems with Hamiltonians $H(\tau)$ which explicitly depend on time $\tau$. Therefore the entire Hilbert space of many-body quantum configurations (Fock space) is dynamically accessible, and the ''microcanonical'' average of an *intensive* or *local* observable, represented by an operator $A$, reads

$$\langle A \rangle = \lim_{L\to\infty} \frac{\text{tr}\,A}{\text{tr}\,1}. \tag{1}$$

If the system possesses a group of exact geometric or dynamical symmetries, the trace in Eq. (1) may be considered only over a specific symmetry class of the Fock space with respect to the symmetry group. For example, if the system is autonomous, $\partial H/\partial\tau\equiv0$, energy is conserved, and Eq. (1) should be replaced by the average over a specific ''energy shell''; or, as often, if the number $N$ of particles (or the particle density $\rho=N/L$) is preserved, then the microcanonical average should be performed over the Fock subspace of fixed density ($N$-particle) configurations

$$\langle A \rangle_\rho = \lim_{L\to\infty} \frac{\text{tr}\,(A\,\delta_{[\rho L],N})}{\text{tr}\,\delta_{[\rho L],N}}, \tag{2}$$

where $[x]$ is an integer part of $x$, and $\delta_{m,n}$ is a standard Kronecker symbol. When we want to keep the size $L$ in average (2) fixed and finite, we write $\langle A \rangle_\rho^L$. Although in this abstract discussion we would like to avoid the notion of temperature [9], one may also think of Eqs. (1) or (2) as canonical averages at very large or infinite temperature, $\beta=(k_BT)^{-1}\to0$.

As we shall often speak about the ''thermodynamic limit'' throughout this paper we must define the precise

meaning of these words: The fact that the property $\mathcal{A}$ is valid in the TL, say that the quantity $\mathcal{F}(L)$ has a value $\mathcal{F}_\infty$, can be understood either (i) in a *weaker* sense, i.e., $\mathcal{F}(L)$ *may* or *may not* be defined for an infinite ($L=\infty$) system but $\mathcal{F}(L)$ approaches $\mathcal{F}_\infty$ as we approach the TL, $\lim_{L\to\infty}\mathcal{F}(L)=\mathcal{F}_\infty$; or (ii) in a *stronger* sense, i.e., the property $\mathcal{A}$ is well defined for an infinite system $L=\infty$, and is therein satisfied. Whenever the property $\mathcal{A}$ is defined for a finite system as well, then (ii) implies (i) and we *will* safely use definition (i). This will be used througout most of the paper (Secs. I–IV), whereas in Sec. V we shall deal with operator algebra over infinite systems and only there may we understand TL with assumption (ii).

The system is defined to be *quantum ergodic* if the time average of *(almost) any observable* in the Heisenberg picture $A(\tau)$ is equal to the microcanonical average $\langle A\rangle$ times a unit operator (over the corresponding desymmetrized Fock subspace)

$$\bar{A} := \lim_{T\to\infty}\frac{1}{T}\int_0^T d\tau A(\tau) = \langle A\rangle 1. \qquad (3)$$

In the case where one has a constant of motion, e.g., a density of particles $\rho = N/L$ (or energy $E=H$, etc.), one should define the ergodicity through the spectral resolution of the relevant invariant operator, $\rho = \int\rho' dE_{\rho'}$, namely,

$$\bar{A} = \int \langle A\rangle_{\rho'} dE_{\rho'}. \qquad (4)$$

When the microcanonical average does not depend on the eigenvalues of the symmetry operations or *quantum numbers*, e.g., when the *spectral function* is a constant, $\langle A\rangle_\rho \equiv \langle A\rangle$, then definition (4) is equivalent to a simple one [Eq. (3)].

In this paper we will consider the case of a *periodic time dependent* Hamiltonian, say with period $p$, $H(\tau+p)=H(\tau)$, where the dynamics is fully described by iterating the *unitary quantum propagator over one period of time*, i.e., the Floquet map which is defined as a time-ordered product $U := \hat{T}\exp[-i\int_0^p d\tau H(\tau)/\hbar]$. In such a case, operator $U$, or any well defined function of it $f(U)$ [10,11], is a conserved quantity, $\overline{f(U)}=f(U)$, and we must use a definition of quantum ergodicity (4) instead of Eq. (3). If $U=\int_{-\pi}^{\pi}e^{-i\varphi}dE_\varphi$ is a spectral resolution of the quasienergy with the spectral parameter $\varphi\in[-\pi,\pi)$, then we should define the quantum ergodicity as

$$\bar{A} = \int_{-\pi}^{\pi}\langle A\rangle_\varphi dE_\varphi \qquad (5)$$

for some spectral function $\langle A\rangle_\varphi$. However, if we restrict ourselves only to such observables $A$, which are "orthogonal" to all nonzero powers of $U$, i.e., which satisfy $\langle AU^n\rangle = 0$, for all $n = \pm 1, \pm 2, \ldots$, then the spectral function is trivial, $\langle A\rangle_\varphi \equiv \langle A\rangle$, and the simple definition (3) applies. In fact, this is true for *almost any* observable in the TL provided that (as we approach the TL, $L$ large but finite) the matrix of the propagator $U$ in an eigenbasis $|a\rangle$ of a generic observable $A$, $A|a\rangle = a|a\rangle$, behaves as a unitary pseudorandom matrix

which belongs to the circular orthogonal or circular unitary ensemble (COE or CUE) [12]. For a finite but increasing size $L$, the dimension of the Fock space $\mathcal{N}=\text{tr}\,1$ is finite and diagonal elements of the Floquet maps $U^n$ are pseudorandom numbers with zero mean and decreasing magnitude, $|\langle a|U^n|a\rangle| = O(\mathcal{N}^{-1/2})$, so we find $\langle AU^n\rangle \sim \langle A\rangle/\mathcal{N} \to 0$ as $L\to\infty$.

Therefore, provided that the Floquet matrix in a generic basis $\langle a|U|a'\rangle$ has a COE or CUE structure, one may argue that the quasienergy becomes irrelevant in the TL, just as it becomes irrelevant in the classical limit ($\hbar\to 0$) of chaotic one-particle and few-particle systems [13,14]. Note that in a specific class of dynamical system a more formal and close analogy between the TL and the (quasi)classical limit has recently been established [15].

However, since we have no *a priori* theoretical arguments to predict COE or CUE structure of the many-body Floquet matrix, we must emphasize that the full Fock space ergodicity (3), as required for almost any obserbable $A$ in the case of periodic time-dependent Hamiltonian is a much *stronger* condition than Eq. (5). Therefore, we stress right at the outset that our numerical results strongly support the full Fock space ergodicity of typical observables in our two-parameter family of quantum many-body dynamical systems, when the integrability breaking parameters are sufficiently large. (See Sec. IV B for a detailed numerical analysis of spectral functions of typical observables, while all the other numerical results in the paper, on quantum mixing and ergodicity in Secs. III and V, respectively, are fully consistent.)

Alternatively, one generally defines quantum ergodicity in a more rigorous but essentially equivalent way [Ref. [16], Eq. (B6)], namely by writing the expectation value of Eq. (3) in an arbitrary *normalized* state $|\psi\rangle$:

$$\lim_{T\to\infty}\frac{1}{T}\int_0^T d\tau\langle\psi|A(\tau)|\psi\rangle = \langle A\rangle. \qquad (6)$$

Quantum ergodicity is now defined [16] by requiring Eq. (6) for *any* observable $A$ and for *(almost) any* pure state $|\psi\rangle$. The phrase *almost* (again) refers to the case of a time-periodic Hamiltonian. The set of states $|\psi\rangle$ for which Eq. (6) may be violated, e.g., the eigenstates of $U$, has a measure zero in the full Fock space in the TL. In such a case, definition (6) is equivalent to the full Fock space ergodicity (3) or, as $L \to\infty$ ($\mathcal{N}\to\infty$), the matrix of $U$ in almost any (generic) Fock space basis looks more and more like a member of an $\mathcal{N}$-dimensional COE or CUE. However, the last definition of quantum ergodicity (6) is somehow more robust than Eq. (3) since observable $A$ may here be completely arbitrary. Even if $A=f(U)$, it is true for almost any state $|\psi\rangle$ that one may consider $\langle\psi|U^n|\psi\rangle$ ($n\neq 0$) as a diagonal element of a unitary pseudorandom matrix which is expected to fluctuate around zero as $O(\mathcal{N}^{-1/2})$, and hence vanishes in the TL ($\mathcal{N}\to\infty$).

An even stronger ergodic property is *quantum mixing*, which is defined very generally according to Refs. [16–18] as follows: A quantum many-body system is called quantum mixing in the TL if the time correlation function of an (almost) arbitrary pair of quantum observables in the Heisenberg representation, i.e., for *(almost) any observable* $A(\tau)$ and for *any observable* $B(\tau)$, decays to zero:

$$C_{AB}(\tau) := \langle A(\tau)B(0) \rangle - \langle A \rangle \langle B \rangle, \quad \lim_{\tau \to \infty} C_{AB}(\tau) = 0. \quad (7)$$

Note that formula (7) implies that the TL ($L \to \infty$) should be considered prior to the time limit, $\tau \to \infty$, since these two limits do not generally commute [18]. Again, in the case of additional symmetry, or conserved (quasi)energy, mixing over separate symmetry classes can be studied, as well as *uniform mixing* over the entire Fock space [which makes sense when the microcanonical averages (spectral functions) of $A$ and $B$ do not depend on quantum numbers or spectral parameters such as $\rho = N/L$, $E$, or $\varphi$].

In Ref. [18] quantum mixing of a system of interacting bosons has been related to a hard chaos of the corresponding classical (mean field) model. However, general quantum systems need not possess the classical limit; when they do, the general definitions (3)–(7) go over to the correct definitions of classical ergodicity and mixing of the corresponding classical counterparts.

It is easy to see that the same implication holds as in the classical mechanics [2]: Quantum mixing (7) implies quantum ergodicity (3). To establish this, observe that, as a simple consequence of Eq. (7), the time-averaged correlation function should vanish:

$$\bar{C}_{AB} := \lim_{T \to \infty} \frac{1}{T} \int_0^T d\tau C_{AB}(\tau) = 0.$$

Assuming that the order of the time average and the micorcanonical average can be interchanged, the last fact is equivalent to

$$\langle \bar{A}B \rangle - \langle A \rangle \langle B \rangle = \langle (\bar{A} - \langle A \rangle 1)B \rangle = 0.$$

From here we immediately see that the observable in brackets should vanish, $\bar{A} - \langle A \rangle 1 = 0$, since observable $B$ is arbitrary. The last argument can be reversed, so we see that quantum ergodicity (3) is equivalent to $\bar{C}_{AB} = 0$ for *almost* arbitrary pair of observables $A, B$.

We expect that quantum mixing implies universal statistical properties of energy spectra (and also universal statistics of occupation numbers [19], matrix elements, etc.) described by random matrix theory [12]. Random matrix spectral statistics have indeed been demonstrated numerically for a few strongly nonintegrable many-body systems [20]. On the other hand, completely integrable quantum many-body systems (having an infinite set of independent conservation laws $Q_n$, $n = 1,2,3 \dots$) are obviously nonergodic ($\overline{Q_n} = Q_n \neq \langle Q \rangle_n 1$), and therefore nonmixing, and are characterized by the universal Poissonian spectral statistics [20].

It has been pointed out recently [21,22] that integrability typically implies nonvanishing stiffness, i.e., ideal (ballistic) transport with infinite transport coefficients (or ideal insulating state). Indeed, there is a direct implication of quantum mixing and quantum ergodicity on quantum transport. One should simply inspect a Kubo formula [23], which relates the real part of the transport coefficient, e.g., electric conductivity $\sigma'(\omega)$, to the cosine transform of the autocorrelation function of the electric current observable $J$, written for high temperatures (small $\beta$) as

$$\sigma'(\omega) = \frac{1}{2}\beta \int_{-\infty}^{\infty} \cos(\omega\tau) \left\langle \frac{1}{L} J(0)J(\tau) \right\rangle d\tau. \quad (8)$$

The transport is diffusive, and the system behaves as a *normal conductor*, if zero-frequency (dc) conductivity is finite, $\sigma'(0) < \infty$, which means that the time integral of the current-current correlation function should be finite; this is true if the system is mixing and if time correlations decay sufficiently fast, e.g., it is sufficient that $|\langle (1/L)J(0)J(\tau) \rangle| < C|\tau|^{-\alpha}$ for some $C > 0$ and $\alpha > 1$.

On the other hand, if the transport is ballistic, dc conductivity diverges $\sigma'(0) = \infty$ and frequency dependent conductivity can be written as a sum of a $\delta$-function spike and a regularized conductivity:

$$\sigma'(\omega) = D\delta(\omega) + \sigma_{\text{reg}}(\omega), \quad D = \lim_{\epsilon \to 0} \int_{-\epsilon}^{\epsilon} \sigma'(\omega)d\omega. \quad (9)$$

The weight $D$ is known as a *charge stiffness* (or Drude weight), and is proportional to the averaged current-current time correlator

$$D = \beta D_J, \quad D_A = \lim_{T \to \infty} \lim_{L \to \infty} \frac{1}{2TL} \int_{-T}^{T} C_{AA}^L(\tau)d\tau. \quad (10)$$

Therefore, the nonvanishing charge stiffness $D_J \neq 0$, meaning a ballistic electronic transport, is a sufficient condition for deviation from quantum ergodicity, so $D_J$ will be extensively used as a quantitative indicator of quantum (non)ergodicity throughout the rest of this paper.

In a generic integrable system one can find an (infinite) set of invariant *extensive* observables, the so-called conserved charges $Q_n$. Mazur [24] and Suzuki [25] proposed a ''Parseval-like'' inequality for the time-averaged autocorrelator of any extensive observable $A$,

$$D_A \geq \sum_n \frac{\left| \left\langle \frac{1}{L}AQ_n \right\rangle \right|^2}{\left\langle \frac{1}{L}Q_n^2 \right\rangle}, \quad (11)$$

using any suitable (sub)set of conserved charges $\{Q_m\}$, such that $\langle (1/L)Q_nQ_m \rangle = 0$ if $n \neq m$. For an integrable system one therefore proves ideal (ballistic) transport ($D_J > 0$) if at least one term in an infinite sum on the right-hand side of Eq. (11) applied to the current observable $A = J$ is nonvanishing (which is typically the case) [22]. It is convenient to say that $\{Q_n\}$ is a *complete* set of conserved charges if Eq. (11) is an exact *equality* for any observable $A$ [which is ''square summable,'' $\langle (1/L)A^2 \rangle < \infty$].

The important and delicate question is whether nonergodicity of an integrable system in the TL can be structurally stable against generic and finite nonintegrable perturbation. In this paper we will present clear numerical evidence based on various different and independent numerical methods in support of a conjecture claiming an affirmative answer to the above question.

**Conjecture:** Let $H_\lambda$ be a continuous family of *generic infinite* quantum many-body systems with *local* interaction

[26], such that $H_0$ is completely integrable while $H_\lambda$ are nonintegrable for almost any $\lambda \neq 0$. Then $\exists \lambda_c$, such that all $H_\lambda$ are *nonergodic* and *nonmixing* for $|\lambda| < \lambda_c$. One important consequence of this conjecture would be a large class of not only completely integrable but also nearly integrable many-body systems for which ideal transport and infinite conductance would be expected.

In should be emphasized that the existence of quasi-integrable dynamics, neither completely integrable nor ergodic, in the TL is also an interesting debated issue in the context of many-body classical mechanics. For example, in the case of a nonintegrable chain of classical anharmonic coupled oscillators (the Fermi-Pasta-Ulam problem), a strong deviation from ergodicity was found long ago [5], and recently shown to imply anomalous classical energy transport [6], which has been only partially explained in terms of standard chaos criteria [8,7]. However, in this paper we consider the problem in a purely quantum setting, in a fermionic or spin-$\frac{1}{2}$ system for which any kind of classical or quasiclassical limit cannot be defined, so the results based on classical dynamics cannot be directly related to our discussion.

In Sec. II we define a two parametric family of generic nonintegrable many-body systems [27], namely, a kicked-parameter $(t,V)$ model of interacting spinless fermions, or equivalently, a kicked Heisenberg $XX$-$Z$ spin-$\frac{1}{2}$ chain, and describe the basic properties of the model. In Sec. III we show how efficient explicit time evolution of the above model of finite but quite large size $L$ can be computed, and present results on extensive numerical computation of time correlation functions. By letting the size $L$ to increase and inspecting TL, we clearly identify two regimes of quantum motion: the *nonmixing* regime for small and intermediate values of kick parameters where time correlation functions typically saturate to constant nonvanishing values, and an *exponentially mixing* regime for sufficiently large values of kick parameters where time correlation functions decay *exponentially*. As a complementary approach to a direct time evolution (time domain) we perform, in Sec. IV, a complete diagonalization of the stationary problem (frequency domain) for finite sizes $L$. Using the stationary data we compute and analyze short- and long-range quasienergy level statistics. By further inspecting a statistical distribution of diagonal matrix elements of three typical observables, we clearly demonstrate the full Fock space ergodicity (3) as we approach the TL for sufficiently large values of the kick parameters, whereas for smaller values of the kick parameters we find a manifestly nonergodic behavior: a nontrivial and nonshrinking (as the size $L$ increases) distribution of diagonal matrix elements around a nonconstant spectral function. By means of off-diagonal matrix elements of the current observable $J$, we directly compute the conductance and the charge stiffness $D_J$. The obtained results are in quantitative agreement with a direct time evolution (Sec. III). In Sec. V we outline a completely different and independent method of computing time-averaged observables and quantitative indicators of quantum ergodicity such as the charge stiffness $D_J$, by making use of extensive computerized Lie algebra. This third method, in contrast to the other two, refers directly to infinite systems (infinite lattices $L = \infty$) and, again, gives compatible results. In Sec. VI we give some additional argu-ments in support of our conjecture by discussing some relevant published and unpublished results, and conclude.

## II. MODEL

No general analytical methods exist to deal with dynamics of nonintegrable quantum many-body systems. A solition theory based on inverse scattering and an algebraic Bethe ansatz [28] is unfortunately applicable only to a limited class of very special, completely integrable many-body systems. Therefore one is led to numerical experiments to learn about the dynamics of generic quantum many-body systems, encouraged by the fact that numerical and experimental investigations of dynamical systems of one or few particles has been a very fruitful area of research (known as quantum chaos) over the past 20 years [13,14]. However, one should be very careful in picking out the toy model, since the fact that the dimensionality of the Hilbert space (Fock space of quantum many-body states) grows exponentially with increasing system size $L$ makes a serious quantitative study of the TL almost prohibitive. Here we propose the simplest many-body system that we can think of: a one-dimensional lattice of spinless fermions of size $L$; for reasons which will become clear in Sec. III, we decide to break integrability by taking a time-dependent interaction which is switched on periodically by means of $\delta$ kicks. Therefore, the time-dependent Hamiltonian of our ''kicked $(t,V)$ model'' (K$tV$) [27] reads

$$H(\tau) = \sum_{j=0}^{L-1} \left[ -\tfrac{1}{2} t(c_j^\dagger c_{j+1} + \text{H.c.}) + \delta_p(\tau) V n_j n_{j+1} \right].$$

$$(12)$$

$c_j^\dagger$ and $c_j$ are fermionic creation and annihilation operators satisfying canonical anticommutation relations, $[c_j, c_k]_+ := c_j c_k + c_k c_j = 0$. $[c_j^\dagger, c_k]_+ = \delta_{jk}$ and $n_j = c_j^\dagger c_j$ are number operators, and periodic boundary conditions are imposed $c_L \equiv c_0$. $\delta_p(\tau) = \sum_{m=-\infty}^{\infty} \delta(\tau - m)$ is a periodic $\delta$ function. We use units in which $\hbar = $ (time between collisions) $ = $ (lattice spacing) $ = 1$. The hopping amplitude $t$ and interaction strength $V$ are independent (kick) parameters. An important and useful property of kicked systems like Eq. (12) is the fact that the evolution propagator over one period (Floquet operator) factorizes into the product of kinetic and potential parts:

$$U = \hat{T} \exp\left( -i \int_{0^+}^{1^+} d\tau H(\tau) \right) = \exp(-iW) \exp(-iT),$$

$$(13)$$

$$T = -\tfrac{1}{2} t \sum_{j=0}^{L-1} (e^{i\phi} c_{j+1}^\dagger c_j + e^{-i\phi} c_j^\dagger c_{j+1}), \qquad (14)$$

$$W = V \sum_{j=0}^{L-1} n_j n_{j+1}. \qquad (15)$$

We have used a Peierls phase $\phi$ in order to introduce a particle current

$$J=(i/t)U^{\dagger}(\partial/\partial\phi)U|_{\phi=0}=\tfrac{1}{2}i\sum_{k=0}^{L-1}(c_j^{\dagger}c_{j+1}-c_{j+1}^{\dagger}c_j) \tag{16}$$

(which is divided by $t$ for convenience); elsewhere we set $\phi:=0$. Note that the kinetic energy $T$ as well as the current $J$ are *diagonal* in momentum representation:

$$T=t\sum_{k=0}^{L-1}(1-\cos(sk))\tilde{n}_k, \tag{17}$$

$$J=\sum_{k=0}^{L-1}\sin(sk)\tilde{n}_k, \tag{18}$$

where $s=2\pi/L$, while the tilde refers to momentum representation of field operators:

$$\tilde{c}_k=L^{-1/2}\sum_{j=0}^{L-1}\exp(isjk)c_j, \quad \tilde{n}_k=\tilde{c}_k^{\dagger}\tilde{c}_k. \tag{19}$$

Using a well known Jordan-Wigner transformation [29] one can map one-dimensional (1D) lattice of spinless fermions to a spin-$\tfrac{1}{2}$ chain described by Pauli operators $\sigma_j^{\pm}=(\sigma_j^x\pm i\sigma_j^y)/\sqrt{2}$ and $\sigma_j^z$, namely,

$$\sigma_j^+=\sqrt{2}c_j^{\dagger}\exp\left(i\pi\sum_{j'=0}^{j-1}n_{j'}\right),$$
$$\sigma_j^z=2n_j-1, \tag{20}$$

which satisfy canonical commutation relations

$$[\sigma_j^{\mu},\sigma_k^{\nu}]=i\sum_{\eta}\epsilon_{\mu\nu\eta}\sigma_j^{\eta}\delta_{jk}, \quad \mu,\nu,\eta\in\{x,y,z\}.$$

In fact, the Jordan-Wigner transformation (20) maps K$tV$ model on a kicked Heisenberg $XX$-$Z$ chain:

$$H(\tau)=T+\delta_p(\tau)W, \tag{21}$$

$$T=\tfrac{1}{4}t\sum_{j=0}^{L-1}(\sigma_j^x\sigma_{j+1}^x+\sigma_j^y\sigma_{j+1}^y), \tag{22}$$

$$W=\tfrac{1}{4}V\sum_{j=0}^{L-1}(\sigma_j^z\sigma_{j+1}^z+2\sigma_j^z). \tag{23}$$

The last term of potential (23) is irrelevant since the total $z$ spin $S_z=\Sigma_{j=0}^{L-1}\sigma_j^z=N-\tfrac{1}{2}L$ is a constant of motion, $[U,S_z]=0$.

Interaction strength $V$ is a *cyclic parameter* $V\equiv V(\mathrm{mod}\,2\pi)$, since the spectrum of $W/V$ is a set of integers [see Eq. (15)]. The K$tV$ model is integrable and solvable in three special (limiting) cases: (1) a $t=0$, 1D Ising model; (2) $V=0(\mathrm{mod}\,2\pi)$, 1D free fermions, or equivalently, a 1D Heisenberg $XX$ $\tfrac{1}{2}$-spin chain; and (3) $tV\rightarrow0$ and $\Delta=t/V$ finite (continuous-time), 1D Heisenberg $XXZ$ $\tfrac{1}{2}$-spin chains.

For $t\neq0$, $V\neq0$ (mod $2\pi$), the K$tV$ model is expected to be nonintegrable, possibly quantum ergodic, and mixing.

To conclude this section, let us list the symmetries of a general K$tV$ model (for arbitrary $t$ and $V$): In addition to the trivial conservation law, namely, the number or density of particles

$$N=\sum_{j=0}^{L-1}n_j, \quad \rho=\frac{N}{L}, \quad [U,N]=0, \tag{24}$$

and the total quasimomentum $K\in\{0,1,\ldots,L-1\}$ which is defined as an eigenvalue of a unitary translational symmetry operation $S$,

$$S=\exp(isK)=\exp\left(is\sum_{k=0}^{L-1}k\tilde{n}_k\right), \quad [U,S]=0, \tag{25}$$

the K$tV$ model has two (geometric) "reflection" symmetries: the *parity* transformation

$$\hat{\mathcal{P}}: \, c_j\rightarrow c_{L-j}, \quad \hat{\mathcal{P}}U=U\hat{\mathcal{P}}, \quad \hat{\mathcal{P}}^2=\hat{1}, \tag{26}$$

and, for even size $L$, the particle-hole transformation

$$\hat{\mathcal{R}}: \, c_j\rightarrow(-1)^jc_j^{\dagger}, \quad \hat{\mathcal{R}}U=U\hat{\mathcal{R}}, \quad \hat{\mathcal{R}}^2=\hat{1}. \tag{27}$$

Note on notation: Symbols wearing a "hat" denote linear transformations over the operator space of quantum observables.

## III. FIRST METHOD: DIRECT TIME EVOLUTION AND CORRELATION FUNCTIONS

For a fixed size $L$ and a fixed number of fermions $N$, a unitary quantum many-body map $U$ [Eq. (13)] acts over a Fock space of dimension

$$\mathcal{N}=\binom{L}{N}=\frac{L!}{N!(L-N)!}. \tag{28}$$

The dynamics of a given initial many-body state $|\psi(0)\rangle$ is a simple iteration of the Floquet map

$$|\psi(m)\rangle=U|\psi(m-1)\rangle=U^m|\psi(0)\rangle. \tag{29}$$

Many-body states $|\psi\rangle$ can be expanded in a complete basis of the Fock space (of Slater determinants), for which we may choose either *position states*, labeled by sets of $N$ ordered integers $\vec{j}=(j_1,\ldots,j_N)$,

$$|\vec{j}\rangle=c_{j_1}\cdots c_{j_N}|0\rangle, \quad 0<j_1<\cdots<j_N<L, \tag{30}$$

or *momentum states*, labeled by sets of $N$ ordered integers $\vec{k}$,

$$|\vec{k}\rangle=\tilde{c}_{k_1}\cdots\tilde{c}_{k_N}|0\rangle, \quad 0<k_1<\cdots<k_N<L. \tag{31}$$

An important observation, implicitly made already in Sec. II, Eqs. (13), (15), and (17), is that the kinetic propagator $\exp(-iT)$ is diagonal in the momentum representation while the potential propagator $\exp(-iW)$ is diagonal in the position representation:

$$U_{\vec{k},\vec{k}'}^T := \langle \vec{k}| \exp(-iT)|\vec{k}'\rangle$$

$$= \delta_{\vec{k},\vec{k}'} \exp\left( it \sum_{n=1}^{N} [\cos(sk_n)-1] \right), \qquad (32)$$

$$U_{\vec{j},\vec{j}'}^W := \langle \vec{j}| \exp(-iW)|\vec{j}'\rangle$$

$$= \delta_{\vec{j},\vec{j}'} \exp\left( -iV \sum_{n,n'=1}^{N} \delta_{j_{n'},j_n+1} \right). \qquad (33)$$

Therefore, one may formulate a very efficient algorithm to perform an explicit time evolution of many-body states, provided that it is possible to switch between the two representations (30) and (31) as efficiently as in the problem of one kicked quantum particle $N=1$, e.g., the kicked rotor [30] or kicked Harper model [31], by means of the fast Fourier transformation (FFT) algorithm. Indeed, we succeeded in developing a fast algorithm which performs such an antisymmetrized multidimensional discrete Fourier transformation

$$F_{\vec{j},\vec{k}} = \langle \vec{j}|\vec{k}\rangle \qquad (34)$$

in roughly $\mathcal{N} \log_2 \mathcal{N}$ floating point operations (FPO's). The algorithm is based on a factorization of an $L$-site discrete Fourier transformation into the product of $\sim L \log_2 L$ two-site transformations parametrized with $2\times 2$ submatrices $(\alpha,\beta;\gamma,\delta)_{jj'}$, which are successively applied to pairs of creation operators, $(c_j^\dagger, c_{j'}^\dagger) \leftarrow (\alpha c_j^\dagger + \beta c_{j'}^\dagger, \gamma c_j^\dagger + \delta c_{j'}^\dagger)$, in all Slater determinants $\Pi_n c_{j_n}^\dagger|0\rangle$ which contain a particle at sites $j$ or $j'$. (One should be careful in dealing with fermionic signs of Slater determinants when sorting the factors in the product $\Pi_n c_{j_n}^\dagger|0\rangle$.) In case when $L=2^p$, factorization of FFT to a chain of two-site (in such case unitary) transformations is easily deduced by inspecting a conventional FFT algorithm (such as the one implemented in Ref. [32]), while for more general lattice sizes [we have so far implemented such a Fermionic FFT (FFFT) algorithm for $L = 10, 12, 15, 20, 24, 30,$ and 40] we factorized the optimal schemes developed by Winograd [33]. Our FFFT algorithm requires almost no extra storage apart from a vector of $\mathcal{N} c$ numbers where the quantum many-body state is stored. Therefore, map (13) is iterated on a vector $\psi_{\vec{k}}(m) = \langle \vec{k}|\psi(m)\rangle$, using the matrix composition

$$U = F^* U^W F U^T \qquad (35)$$

in roughly $2\mathcal{N}\log_2 \mathcal{N}$ FPO's per time step, which is by far superior to ''brute-force'' methods based on complete diagonalization of $U$ and expansion of time-evolving state $|\psi(m)\rangle$ in terms of eigenstates of $U$.

Let us now consider the time autocorrelation functions of two ''generic'' observables, namely, the current $J$ and rescaled traceless kinetic energy $T'$:

$$C_J^L(m) := \frac{1}{L}\langle J(0)J(m)\rangle_\rho^L$$

$$\qquad (36)$$

$$C_T^L(m) := \frac{1}{L}\langle T'(0)T'(m)\rangle_\rho^L, \qquad T' = \frac{1}{t}T - N$$

where $J(m) = U^{\dagger m}J U^m$ and $T'(m) = U^{\dagger m}T'U^m$. Note that $\langle J\rangle_\rho^L = \langle T'\rangle_\rho^L = 0$. These two observables belong to different symmetry classes with respect to the parity operation

$$\hat{\mathcal{P}}J = -J\hat{\mathcal{P}}, \quad \hat{\mathcal{P}}T' = T'\hat{\mathcal{P}}, \qquad (37)$$

so we choose both to check whether many-body dynamics may depend on the symmetry class with respect to generic ''reflection'' symmetry. Conveniently, both observables $J$ and $T'$ are diagonal in momentum representation,

$$J|\vec{k}\rangle = J_{\vec{k}}|\vec{k}\rangle, \quad J_{\vec{k}} = \sum_{n=1}^{N} \sin(sk_n), \qquad (38)$$

$$T'|\vec{k}\rangle = T'_{\vec{k}}|\vec{k}\rangle, \quad T'_{\vec{k}} = -\sum_{n=1}^{N} \cos(sk_n), \qquad (39)$$

so the time autocorrelation functions can be computed from the time evolution of a (complete) set of $\mathcal{N}'$ $(=\mathcal{N})$ initial momentum states $\vec{k}'$,

$$C_A(m) = \frac{1}{L\mathcal{N}'} \sum_{\vec{k}'}^{'} A_{\vec{k}'} \sum_{\vec{k}} A_{\vec{k}} p_{\vec{k}\vec{k}'}(m), \qquad (40)$$

where $A$ is any observable which is diagonal in momentum basis (here either $J$ or $T'$), and

$$p_{\vec{k}\vec{k}'}(m) = |\langle \vec{k}|\psi(m)\rangle|^2 = |\langle \vec{k}|U^m|\vec{k}'\rangle|^2. \qquad (41)$$

When the dimensionality $\mathcal{N}$ becomes prohibitively large, we suggest estimating the microcanonical averages (36) by taking a smaller $1 \ll \mathcal{N}' \ll \mathcal{N}$ but uniformly random sample of $\mathcal{N}'$ initial states $|\vec{k}'\rangle$, $\langle \cdot \rangle = (1/\mathcal{N}')\Sigma_{\vec{k}'}^{'} \langle \vec{k}'| \cdot |\vec{k}'\rangle (1 + O(1/\sqrt{\mathcal{N}'}))$. Therefore, numerical computation of the correlation function $C_A(m)$ for $m=1,\ldots,M$ can be performed in $\sim (2M\mathcal{N}'\mathcal{N}\log_2 \mathcal{N})/L$ FPO's. Reduction for a factor $1/L$ with respect to a naive FPO count is due to translational symmetry (25), since one can simultaneously simulate the dynamics of $L$ different states with different values of the conserved total momentum $K = \Sigma_{n=1}^N k'_n (\text{mod } L)$.

Let us for the time being fix the density of particles $\rho = N/L = 1/4$. We have performed extensive numerical computations of time correlation functions [by means of explicit time evolution (40)], for sizes $L=8, 12, 16, 20, 24,$ and 32 (at $L=32$ the dimensionality of the Fock subspace is $\mathcal{N} = 10\,518\,300$), and systematically scanned the parameter space $(t,V)$. We have clearly identified two regimes where we were able to probe the TL, i.e., where time correlation functions turned out to be stable against the variation of the system size $L$:

(i) The quantum ergodic and mixing regime for sufficiently large values of parameter $t$ and for any value of parameter $V$ [away from the ''integrable axis'' $V = 0 (\text{mod } 2\pi)$]. In this regime, time correlation functions are rapidly decreasing (case $t=V=4$ is shown in Fig. 1). However, for a finite size $L$ the quantum system is almost never mixing, so correlation functions saturate, on a time scale $\mu(L)$, to a small but nonvanishing value of the stiffness
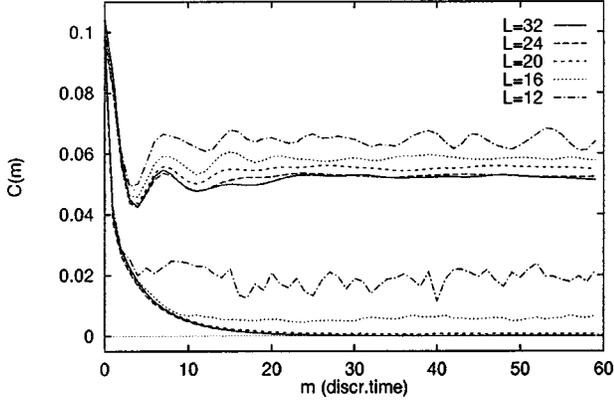
FIG. 1. Current autocorrelation function $C_J(m)$ against discrete time $m$ for quantum ergodic ($t=V=4$, lower set of curves for various sizes $L$) and intermediate ($t=V=1$, upper set of curves) regimes, with density $\rho=\frac{1}{4}$. Averaging over the entire Fock space is performed, $\mathcal{N}'=\mathcal{N}$, for $L\leq 20$, whereas random samples of $\mathcal{N}'=12\,000$ and $800$ initial states have been used for $L=24$ and $32$, respectively.

$$D_A^L = \lim_{M\to\infty} \frac{1}{2M+1} \sum_{m=-M}^{M} C_A^L(m). \qquad (42)$$

(Here $A=J$ or $T'$.) In order to avoid transient behavior at small times $m$ and incorporating the time reversal symmetry, $C_A^L(m)=C_A^L(-m)$, time averages like Eq. (42) have been numerically estimated as $D_A^L=[1/(M'+1)]\Sigma_{m=M'}^{2M'}C_A^L(m)$. Sufficiently large averaging time scale $\{M',\ldots,2M'\}=\{30,\ldots,60\}$ for all sizes $L\leq 32$ (and for most values of parameters $t,V$) has been determined by direct inspection of the correlation functions (see Fig. 1). In Fig. 2 we plot correlation functions $C_J^L(m)$ for $t=V=4$ on a semilog scale, and show that, as the size $L$ is increased, the saturation (or Thouless) time scale $\mu(L)$ increases, roughly as $\mu(L)\sim L$. So the Thouless time $\mu(L)$ clearly diverges in the TL. Fur-
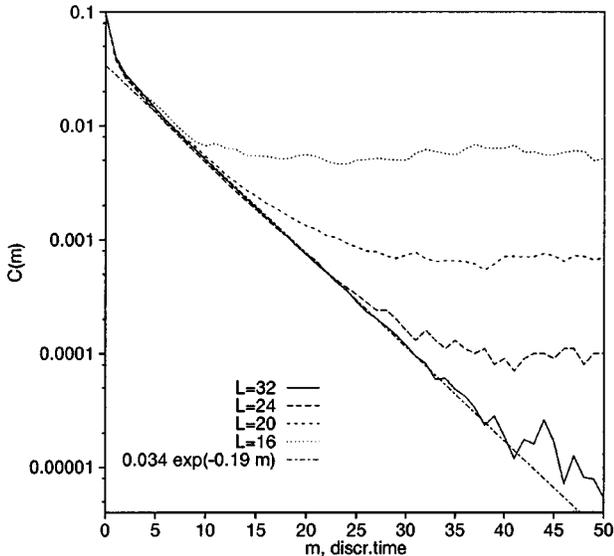


FIG. 2. The lower set of curves ($t=V=4$) of Fig. 1 on semilog scale. To emphasize the exponential correlation decay, we also plot the best exponential fit to the tail of $C_J^{L=32}(m)$ (dash-dotted line).
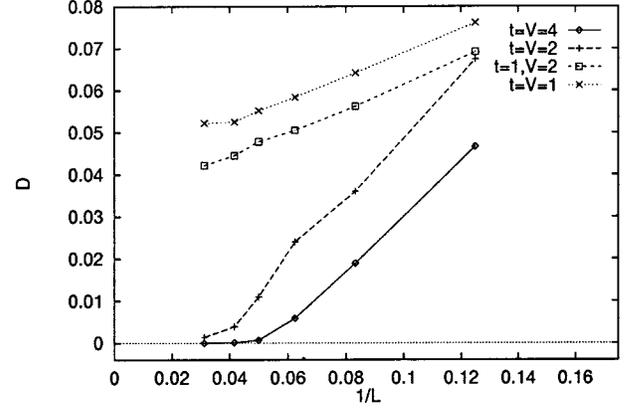


FIG. 3. Stiffness $D_J$ vs $1/L$ at a constant density $\rho=\frac{1}{4}$ and for different values of control parameters in quantum mixing, ergodic regime, $t=V=4$ and $t=V=2$, and the intermediate regimes, $t=1$, $V=2$ and $t=V=1$. Other parameters are the same as in Fig. 1.

thermore, Fig. 2 gives clear numerical evidence (further supported by results shown in Figs. 4 and 5) of the *exponential* decay of time correlation functions in TL [or for times smaller than $\mu(L)$ in a system of finite size $L$]:

$$C_A(m)\propto \exp(-\lambda_A m), \quad m\gg 1. \qquad (43)$$

Henceforth, the stiffness should also vanish exponentially, $D_A^L\sim\exp(-\lambda_A L)$, as one approaches the TL (such behavior was also observed in Ref. [21], indicating exponential mixing in the system sudied there [21]). Indeed, in Fig. 3 we examine $1/L$ scaling of the charge stiffness $D_J^L$ which is (shown here for $t=V=4$ and $t=V=2$) a clear indication of ergodic and mixing behavior in the TL, $D_J^\infty=0$. In this regime, in the TL, Kubo conductivity $\sigma'(\omega=0)=\frac{1}{2}\beta\Sigma_{m=-\infty}^{\infty}C_J(m)$ is finite, $\sigma'(0)<\infty$, and the transport is dissipative. Further, as shown in Ref. [27], the time-averaged current of the arbitrary initial momentum state $|\vec{k}'\rangle$ averages to zero $\bar{J}_{\vec{k}'}=\lim_{M\to\infty}(1/M)\Sigma_{m=1}^{M}\langle\vec{k}'|J(m)|\vec{k}'\rangle=0$, and the aribtrary initial momentum state $|\vec{k}'\rangle$ explores the entire accessible Fock space; i.e., $\langle\vec{k}|U^m|\vec{k}'\rangle$ are uniformly Gaussian pseudorandom numbers when the discrete time $m$ is sufficiently large, say larger than the quantum mixing time.
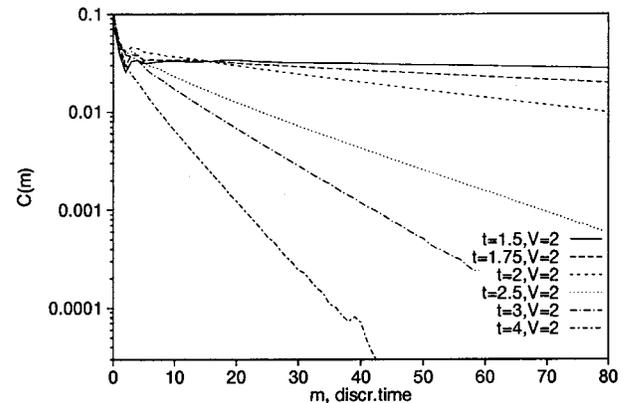


FIG. 4. Current autocorrelation functions $C_J^{L=32}(m)$ for different values of the parameter $t$ (see legend) and a fixed value of the parameter $V$. $\rho=1/4$.
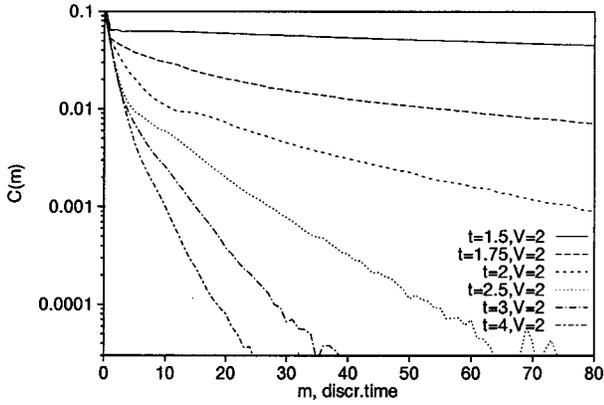
FIG. 5. Kinetic autocorrelation functions $C_T^{L=32}(m)$ for different values of the parameter $t$ (see legend) and a fixed value of the parameter $V$. $\rho = 1/4$. Note that the same scale is used as in Fig. 4.

(ii) Nonergodic and nonmixing regime for parameter $t$ $\sim 1$ (or smaller) and for any value of the cyclic parameter $V$. Here time correlation functions $C_A(m)$ do not decay to zero but saturate, around a constant nonvanishing and typically positive value of the stiffness $D_A^L > 0$ (42), on a short time scale which *does not* depend on the size $L$ (for sufficiently large size $L$). In Fig. 1 we plot the time correlation functions $C_J(m)$ for $t = V = 1$. Please observe the very weak dependence on the size $L$. In Fig. 3 we also show the $1/L$ scaling of the charge stiffness $D_J^L$ for the cases $t = V = 1$ and $t = 1$ and $V = 2$, which clearly indicate a finite extrapolated (to $1/L = 0$) thermodynamic value of the stiffness. This should be considered as evidence of nonmixing and nonergodic behaviors in TL. Since in this parameter ranges the K$t$V model is also noninrtegrable, we will refer to this regime as *intermediate quantum dynamics*. This behavior corresponds to ideal, ballistic transport with an infinite Kubo conductivity $\sigma = \infty$. Furthermore, in Ref. [27] it was shown that in this intermediate regime the time-averaged (persistent) current is *nonvanishing* and *proportional* to the initial current $J_{\vec{k}'}$, $\bar{J}_{\vec{k}'} = \alpha J_{\vec{k}'}$, $\alpha = 2D_J/[\rho(1-\rho)]$ (which is the most direct probe of ideal, ballistic transport), and that an arbitrary time-evolving initial momentum state $U^m|\vec{k}'\rangle$ remains strongly *localized* in a nontrivial subregion of dynamically accessible Fock space.

One may use a charge stiffness of an infinite system $D_J^\infty$ as an order parameter controlling the *dynamical phase transition* from a disordered phase (quantum ergodic and mixing dynamics) characterized by $D_J^\infty = 0$ to an ordered phase (nonergodic and nonmixing dynamics) characterized by $D_J^\infty > 0$. The transition point is characterized by diverging correlation time (or mixing time) scale, $\lambda_J^{-1}$, which diverges when one approaches the transition from above, say, with parameter $t$ decreasing toward a certain critical curve $t_c(V)$. Of course, in the ordered phase, $t < t_c(V)$ and $D_J^\infty > 0$, the time correlations have an infinite range, $C_A(\infty) \neq 0$. The transition is illustrated in Figs. 4 and 5 by plotting correlation functions for both observables, $C_J(m)$ (Fig. 4) and $C_T(m)$ (Fig. 5), for different values of parameter $t$ and fixed parameter $V = 2$. The estimate of the critical parameter here is $1.4 < t_c(V=2) < 1.5$. Observe the *exponential* decay of cor-

relations in all cases, except possibly at very small times where other, smaller time scales may become important.

## IV. SECOND METHOD: EXACT DIAGONALIZATION OF STATIONARY PROBLEM OF FINITE SIZE

In a more complete but brute-force approach, one may try to diagonalize the matrix of a one-period evolution (Floquet) propagator $U$ exactly for a finite size $L$, and compute interesting dynamical quantities, such as conductivity $\sigma'(\omega)$ and stiffness $D_A^L$, directly from the spectrum $\{\varphi_n\}$ and the set of eigenstates $\{|n\rangle\}$ of the K$t$V map $U$:

$$U|n\rangle = \exp(-i\varphi_n)|n\rangle, \quad n = 1 \dots \mathcal{N}. \quad (44)$$

Again, it is easiest to work in the momentum basis (31) and to use the translational symmetry to decompose the matrix $U_{\vec{k},\vec{k}'}$ into blocks (with a fixed value of the total quasi-momentum $K$) of dimension $\mathcal{N}_K \approx \mathcal{N}/L$. Only for blocks with $K = 0$ and $K = L/2$ (if $L$ is even) does the parity operation $\hat{\mathcal{P}}$ (26) commute with the translation $S$ [Eq. (25)], and it may be then used to reduce the dimensionality of the irreducible block further by a factor 2. The matrix $U_{\vec{k},\vec{k}'}$ (for fixed $K$) has been computed, by means of a decomposition (35) and the FFFT algorithm, in roughly a $(\mathcal{N}/L)^2 \log_2 \mathcal{N}$ FPO, and further diagonalized by means of standard routines in roughly a $(\mathcal{N}/L)^3$ FPO, yielding a set of quasienergies $\{\varphi_n\}$ and eigenstates $\langle \vec{k}|n\rangle$.

### A. Spectral statistics

In the so-called quantum chaology of simple (few) body nonintegrable system there is a famous conjecture due to Bohigas, Giannoni, and Schmit [34], supported by numerous numerical [35] and theoretical arguments [36], claiming that hard chaos (ergodicity, mixing, and positive Lyapunov exponents) of a classical counterpart results in universal statistical properties of a system's (quasi)energy spectrum given by the appropriate ensemble of random matrices [12]. On the other hand, integrable classical dynamics results in universal Poissonian statistics of (locally) uncorrelated (quasi)energy levels [37]. Intermediate statistics, which are neither random matrix theory (RMT) nor Poissonian, are found [38,39] for systems whose classical dynamics is intermediate (mixed) with regular and chaotic motion coexisting in phase space. The connection between integrability and nonintegrability and statistics was recently investigated in a few well known examples of nonlinear many-body systems (correlated fermions or interacting spin chains) which do not possess a well defined classical limit [20]. It has been shown that quantum integrability, or (strong) nonintegrability, of the quantum many-body model again correspond to Poissonian, or RMT, behavior of level statistics, respectively. No attempt has been made there [20], however, to understand the intermediate situation, or the thermodynamic limit.

Inspired by quantum chaos, we analyzed the statistical properties of the quasienergy spectrum $\{\varphi_n\}$ of the K$t$V model, and searched for signatures of ergodicity and mixing of the underlying quantum many-body dynamics in the TL. For comparison with other results, the density will be again fixed to $\rho = 1/4$ in the numerical presentation which follows.

First we have analyzed the common short-range statistic, namely, the integrated (cumulative) nearest neighbor level spacing distribution $W(S)$, giving the probability that a random normalized spacing between two adjacent eigenphases $S_n = (\mathcal{N}/2\pi L)(\varphi_{n+1} - \varphi_n)$ is smaller than $S$:

$$W(S) = \frac{1}{\mathcal{N}'} \sum_n{}' \theta(S - S_n). \qquad (45)$$

For moderate values of the size $L \lesssim 20$, the average in Eq. (45) has been computed over all $\mathcal{N}' = \mathcal{N}$ states from all $L$ blocks (symmetry classes) which are labeled by the value of the total quasimomentum $K$. (Note that blocks for $K = K'$ and $K = L - K'$ are related by a parity transformation (26), and give identical (sub)spectra, so one has to diagonalize only $[L/2 + 1]$ different blocks of matrix $U_{\vec{k},\vec{k}'}^{\pm}$.) However, for a larger size $L = 24$ we already have $\mathcal{N}_K \approx 5608$, so we averaged only over one class of fixed quasimomentum, namely, $K = 1$, $\mathcal{N}' = \mathcal{N}_1 \approx \mathcal{N}/L$. (We have carefully checked that the statistical properties of partial subspectra are independent of the symmetry class labeled by the quasimomentum $K$.)

In Fig. 6(a) we show $W(S)$ for size $L = 24$ and several different values of parameter $t$ (and fixed $V = 2$), covering the transition from nonergodic to ergodic and mixing quantum dynamics. We find an almost Poissonian behavior $W_P(S) = 1 - \exp(-S)$ for small $t$ and excellent RMT behavior $W_{\mathrm{COE}}(S) = 1 - \exp(-\pi S^2/4)$ (the Wigner surmise approximating the statistics of the infinitely dimensional circular orthogonal ensemble (COE) [12], due to time-reversal symmetry) for $t > t_c(V)$. In the (more interesting) region of intermediate dynamics $1 \sim t < t_c(V)$ we find intermediate statistics interpolating between Poissonian and COE (see Fig. 6). Interestingly, the level statistics close to the critical point (for $t = 1.4, V = 2$) seems to be well captured by the so-called semi-Poisson model $W_{\mathrm{SP}}(S) = 1 - (1 + 2S)\exp(-2S)$ [40] which has been recently used to model the critical level statistics of 3D Anderson model [41]. Since it is impossible to make statements about the TL of level statistics based on results for a fixed size $L = 24$, in Fig. 6(b) we show the dependence of $W(S)$ on the size $L$ for fixed parameters $t = 1$ and $V = 2$ (in the regime of nonergodic dynamics). Although the intermediate $W(S)$ statistic is closer to Poissonian than to COE, it is being shifted slightly closer to COE as we approach the TL (increase the size $L$), especially in the region of small spacings $S$. This increase of level repulsion as we approach the TL eliminates possible fears of accidental integrability of K$t$V model in the claimed intermediate regime.

Second, we have analyzed the long-range spectral statistics, namely, the number variance

$$\Sigma^2(S) = \langle n(S)^2 \rangle - S^2, \qquad (46)$$

giving the variance of the number $n(S)$ of normalized (unfolded) levels $(\mathcal{N}/2\pi L)\varphi_n$ in a randomly chosen interval of length $S$. [Note that $\langle n(S) \rangle = S$.] For Poissonian and COE models we expect $\Sigma^2_P(S) = S$ and $\Sigma^2_{\mathrm{COE}}(S) \approx (2/\pi^2)\ln(2\pi S)$, respectively. Here, one should note huge degeneracies in the integrable limit $t = 0$ of the Ising model (which are quite common in integrable quantum many-body models in general). For small kick parameters $t$, we hence find stronger-
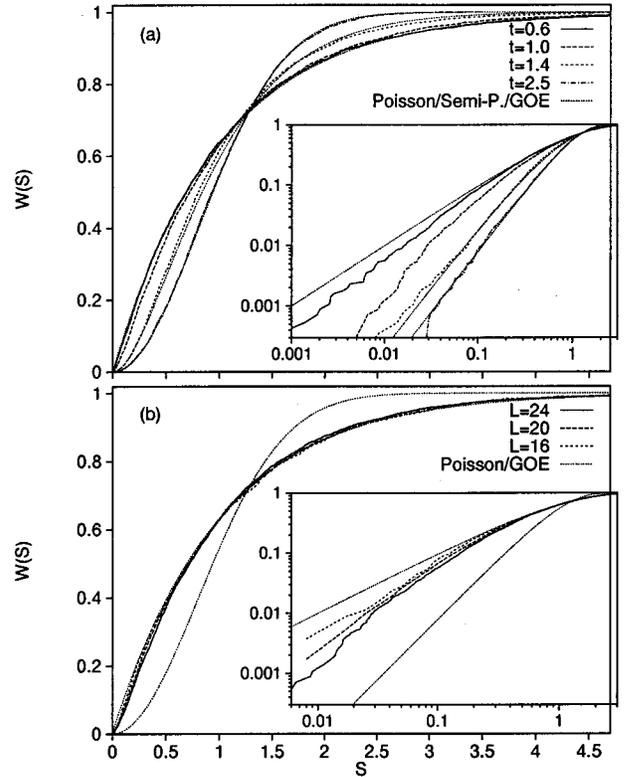


FIG. 6. Cumulative quasilevel spacing distributions $W(S)$ for a quarter-filled $\rho = 1/4$ K$t$V model. In (a) we plot $W(S)$ for several different values of parameter $t$ and fixed parameter $V$ (see legend) covering the mixing and nonmixing transition, and for maximal computable size $L = 24$. With dotted curves we plot, for comparison, the theoretical, Poissonian, semi-Poissonian, and Wigner (COE), distributions. In (b) we show $W(S)$ for fixed kick parameters $t = 1$ and $V = 2$, and for different sizes $L = 16, 20$, and 24. In the insets we plot the same objects on a log-log scale to emphasize the small spacing behavior. Please observe the trend toward linear repulsion [quadratic for $W(S \to 0) \propto S^2$], even in the intermediate regime.

than-Poissonian-level clustering causing faster-than-linear growth of $\Sigma^2(S)$ [Fig. 7(a)]. For finite size $L = 24$, strong level clustering affects also long-range statistics in the regime with mixing dynamics in TL; that is, for $t = 2.5$ we find good agreement with COE statistics only for relatively small spectral ranges $S \lesssim S_{\max} \sim 10^1$. It has been checked, however, that the agreement with COE improves to hold on longer quasienergy ranges ($S_{\max}$ increases), as either the kick parameter $t$ or the size $L$ are increased. In the intermediate regime $1 \sim t < t_c(V)$, the number variance approaches that of an uncorrelated sequence, $\Sigma^2(S) \sim S$, as we approach the TL [see Fig. 7(b) for the case $t = 1$ and $V = 2$]. However, for finite $L$, the phenomenon of saturation sets in, see Ref. [42], namely when the scaled energy range $S = S^*$ is of the order of the density of states,

$$S^* = 0.5\mathcal{N}/L, \qquad (47)$$

i.e., when the energy range $S^*$ becomes comparable to the length of quasienergy spectrum. The numerical factor 0.5 in Eq. (47) is of phenomenological origin. Indeed for data of Fig. 7, for $L = 12, 16, 20$, and 24, the maxima of the number
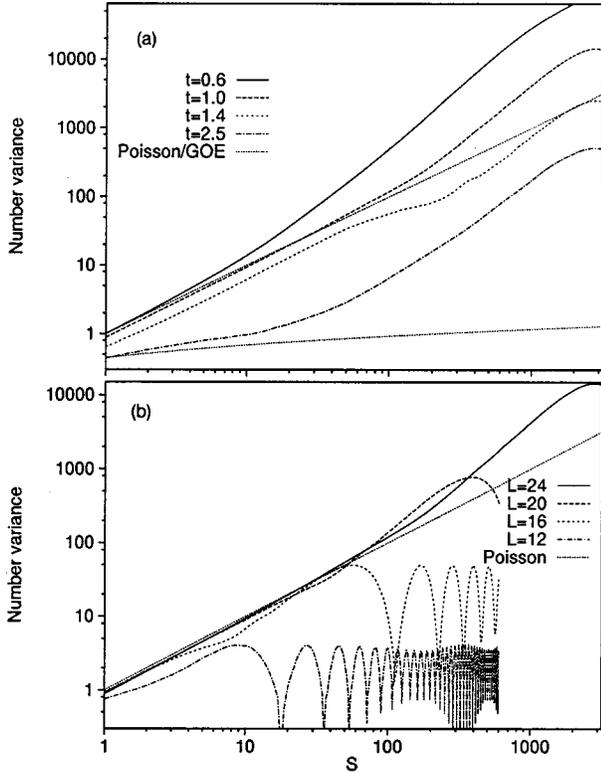
FIG. 7. Number variance $\Sigma^2(S)$ on a log-log scale for exactly the same parameters [with an extra data in (b) for $L=12$] as in Fig. 6.
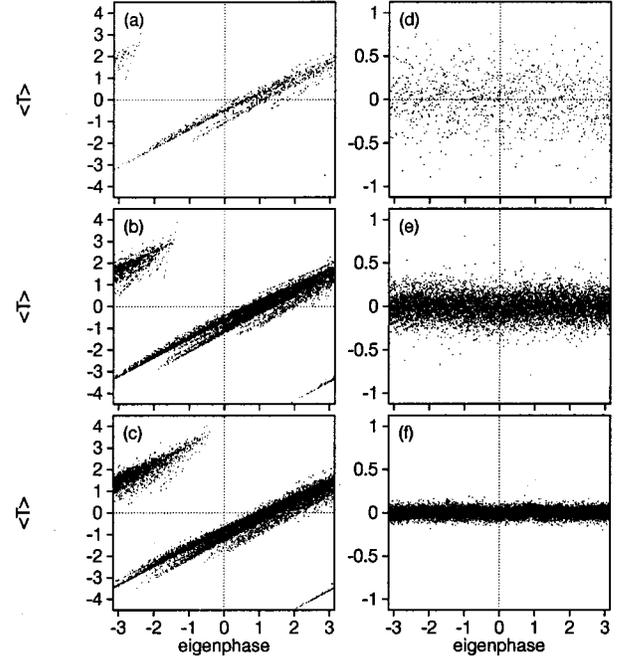


FIG. 8. Diagonal matrix elements of kinetic energy $\langle n|T'|n\rangle$ vs the eigenphase $\varphi_n$, in the intermediate regime ($t=V=1$), (a) for $L=16$, (b) for $L=20$, and (c) for $L=24$, and in the quantum ergodic regime ($t=V=4$), (d) for $L=16$, (e) for $L=20$, and (f) for $L=24$. Note that the ordinate scale is inflated by a factor 4 in the quantum ergodic regime [(d)–(f)].

variance lie at 9, 55, 390, and 2800, whereas theoretical values of $S^*$ [Eq. (47)] are 9.1, 56.9, 387.5, 2804, respectively.

### B. Diagonal matrix elements, spectral functions, and quantum ergodicity

In this subsection we will analyze the statistical distribution of diagonal matrix elements of a few typical observables, in particular as a function of the spectral parameter—the quasienergy $\varphi_n$—in order to understand the typical behavior of the spectral functions and the nature of quantum ergodicity as discussed in Sec. I. Here we consider three typical observables, namely, the particle current $J$ [Eqs. (16) and (38)], the traceless kinetic energy $T'$ [Eqs. (14) and (39)], and the potential energy $W$ [Eq. (15)]. The first two are diagonal in the momentum basis, so their diagonal matrix elements are calculated using the set of eigenstates in the momentum basis, $\langle n|J|n\rangle=\Sigma_{\vec{k}}J_{\vec{k}}|\langle\vec{k}|n\rangle|^2$, whereas the potential operator $W$ is diagonal in the position basis, so we first use FFFT (34) in order to transform the eigenstates from momentum to position basis $\langle\vec{j}|n\rangle=\Sigma_{\vec{k}}F_{\vec{j},\vec{k}}\langle\vec{k}|n\rangle$, and then use the formula $\langle n|W|n\rangle=\Sigma_{\vec{j}}W_{\vec{j}}|\langle\vec{j}|n\rangle|^2$, where $W_{\vec{j}}=V\Sigma_{n,n'}\delta_{j_{n'},j_n+1}$.

We again consider the regime of intermediate dynamics at $t=V=1$ and the strongly nonintegrable regime of presumably ergodic and mixing dynamics at $t=V=4$, both at a particle density $\rho=1/4$. In Figs. 8(a)–8(c) we plot the scatter diagram of diagonal matrix elements of the kinetic energy $\langle n|T'|n\rangle$ vs the value of the quasi-energy $\varphi_n$, for three different system sizes $L=16$, 20, and 24. For $L=16$ and 20, we

superimpose the data for all the symmetry classes labeled by the values of the total quasimomentum $0\leq K<L$, whereas for $L=24$ we compute diagonal matrix elements only for two blocks with total quasimomentum $K=1$ and 5, and carefully check that the results do not depend on $K$. We note that the distribution of points $(\varphi_n,\langle n|T'|n\rangle)$ on the cylinder $[-\pi,\pi)\times\mathbb{R}$ is nontrivial and fairly stable against the variation of the size $L$ (perhaps it is a multifractal, but the statistics is here too poor to investigate this question in more detail). The points $(\varphi_n,\langle n|T'|n\rangle)$ do not seem to converge to the spectral curve $(\varphi,\langle T\rangle_\varphi)$ as $L\to\infty$, where the spectral function $\langle T\rangle_\varphi$ should be determined in general as an average of diagonal matrix elements $\langle n|T'|n\rangle$ in a narrow quasienergy interval

$$\langle T\rangle_\varphi=\lim_{\delta\to 0}\lim_{L\to\infty}\frac{\overset{|\varphi_n-\varphi|<\delta}{\underset{n}{\sum}}\langle n|T'|n\rangle}{\overset{|\varphi_n-\varphi|<\delta}{\underset{n}{\sum}}1}, \qquad (48)$$

where the order of the limits is cruicial, of course. In Fig. 9 we show the overall distribution of diagonal matrix elements $d\mathcal{P}/d\langle n|T'|n\rangle$ and in Table I we give the widths of such distributions, namely, the standard deviations $\sigma_A$ of distributions of diagonal matrix elements of all the three observables $A\in\{J,T',W\}$, which are defined simply as $\sigma_A^2=(1/\mathcal{N})\Sigma_{n=1}^{\mathcal{N}}(\langle n|A|n\rangle-\langle A\rangle)^2$. In this intermediate regime we find that the widths $\sigma_A$ are stable (or even slightly increase) as we increase the size $L$, which is incompatible with
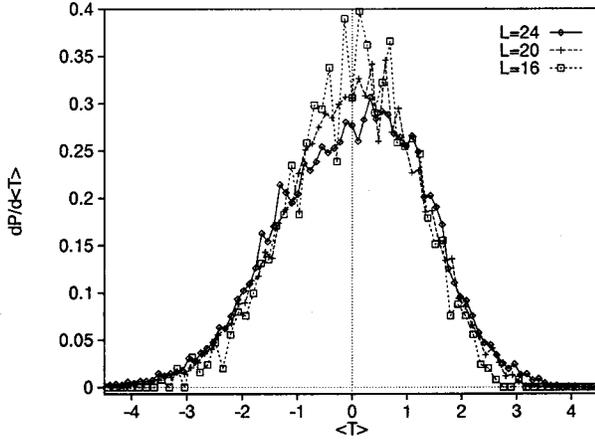
FIG. 9. The distribution of diagonal matrix elements of the kinetic energy $\langle n|T'|n \rangle$ in the regime of intermediate dynamics ($t = V = 1$) for three different sizes $L = 16$, 20, and 24.

any of the two definitions of quantum ergodicity [Eqs. (3) and (5)]. Note that in the completely integrable case, say if $V = 0$, the width of the distribution of diagonal matrix elements can be calculated analytically, since then [27] $\sigma_{T'}^2 = \sigma_J^2 = \langle J^2 \rangle = N(L-N)/(2L-2) = \frac{1}{2}\rho(1-\rho)L + O(1)$, so the width even diverges as $\sim \sqrt{L}$ in TL.

On the other hand, the situation is completely different for substantially larger kick parameters, say for $t = V = 4$, where the system exhibits uniformly mixing behavior as investigated in Sec. III. In Figs. 8(d)–8(f) we show that the scattering of diagonal matrix elements $\langle n|T'|n \rangle$ around the microcanonical average $\langle T' \rangle = 0$ is uniform (independent of the value of the quasienergy $\varphi_n$) and that the width of the swarm of points strongly decreases as the size $L$ increases. Further, we show in Fig. 10 that the distribution of diagonal matrix elements $\langle n|T'|n \rangle$ is in a very good agreement with a *Gaussian*. This finding also supports the hypothesis that $\langle \vec{k}|n \rangle$ are statistically equivalent to the eigenstates of a circular random matrix. The width of the Gaussian distribution decreases with increasing size $L$, and we expect that the scaling with size $L$ should be universal for any spatially homogeneous observable $A$, $[A,S] = 0$, namely,

$$\sigma_A = \text{const} \times \frac{L}{\mathcal{N}}, \quad \mathcal{N} = \binom{L}{N}. \tag{49}$$

This scaling law is derived from a simple assumption that each quasimomentum block of the matrix $\langle n|A|n' \rangle$ is a $\mathcal{N}_K \approx \mathcal{N}/L$-dimensional GOE matrix with the variance which is determined from the constraint $\langle A^2 \rangle / L = O(1)$ that is true for

TABLE I. Standard deviations of the diagonal matrix elements of the three observables $J$, $T'$, and $W$, in the regime of intermediate ($t = V = 1$) and ergodic ($t = V = 4$) dynamics.

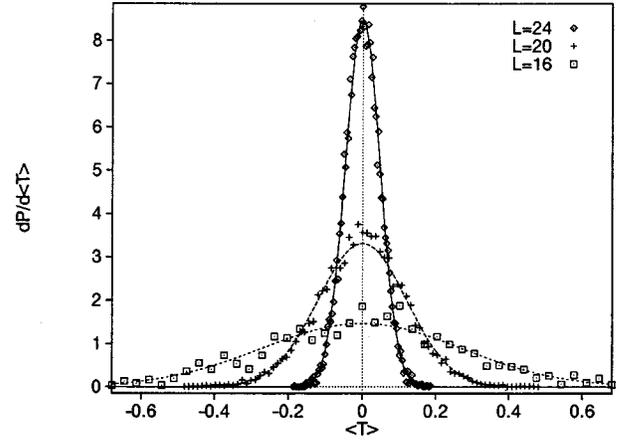| | $t=1$ | $V=1$ | | $t=4$ | $V=4$ | |
| --- | --- | --- | --- | --- | --- | --- |
| $L$ | $\sigma_J$ | $\sigma_{T'}$ | $\sigma_W$ | $\sigma_J$ | $\sigma_{T'}$ | $\sigma_W$ |
| 16 | 0.8927 | 1.1056 | 0.4437 | 0.3212 | 0.2720 | 0.5536 |
| 20 | 0.9647 | 1.2178 | 0.4955 | 0.1495 | 0.1203 | 0.2507 |
| 24 | 1.0430 | 1.3185 | 0.5347 | 0.0628 | 0.0467 | 0.0973 |



FIG. 10. The distribution of diagonal matrix elements of the kinetic energy $\langle n|T'|n \rangle$ in the regime of ergodic dynamics ($t = V = 4$) for three different sizes $L = 16, 20$, and 24. The smooth curves are the best fitting Gaussians (the widths are given in Table I).

any observable of the form $A = \Sigma_j a_j$ where $a_j$ is some local operator density, for example $\langle J^2 \rangle / L = \langle T'^2 \rangle / L \approx \frac{1}{2}\rho(1-\rho)$ [27]. One may check that all the last three columns of Table I indeed obey scaling (49).

Therefore, our numerical results strongly support the full Fock space ergodicity of the $KtV$ model for sufficiently large values of the kick parameters, since for all the three typical observables that we have considered, the spectral function is a constant $\langle A \rangle_\varphi \equiv \langle A \rangle$, and a randomly chosen diagonal matrix element $\langle n|A|n \rangle$ would lie within arbitrarily small distance from the microcanonical average $\langle A \rangle$ for sufficiently large size $L$.

### C. Off-diagonal matrix elements and integrated conductance

From the complete set of eigenstates in the momentum representation, $\langle \vec{k}|n \rangle$, it is also easy to compute the off-diagonal matrix elements of the current observable

$$\langle n|J|m \rangle = \sum_{\vec{k}} J_{\vec{k}} \langle n|\vec{k} \rangle \langle \vec{k}|m \rangle. \tag{50}$$

Again, one should make use of translational symmetry (25), since $[S,J] = 0$, to point out that matrix elements are nonvanishing only within a fixed quasimomentum block, $K_n \neq K_m \Rightarrow \langle n|J|m \rangle = 0$. In order to obtain the numerical results presented in this subsection we have averaged over the entire Fock space (all $K$), except again for $L = 24$ and $\rho = 1/4$, where we have averaged only over a block with quasimomentum $K = 1$. The real part of high-temperature electric conductivity (8) can be (for fixed size $L$) rewritten as

$$\sigma'(\omega) = \frac{\pi\beta}{L\mathcal{N}} \sum_{n,m}^{n \neq m} |\langle n|J|m \rangle|^2 \delta_p\left(\frac{1}{2\pi}(\omega - \phi_m + \phi_n)\right). \tag{51}$$

In order to avoid an awkward smoothing procedure, and to simplify the notation, we introduce a scaled integrated conductivity $I^L(\omega)$,
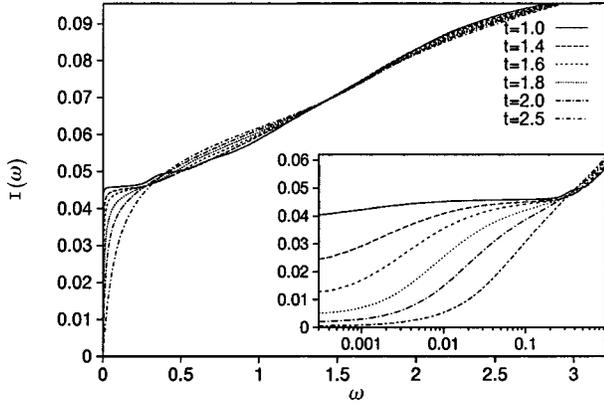
FIG. 11. We show the integrated conductance $I^L(\omega)$ for a cyclic chain of size $L=24$ and parameter $V=2$, and for several different values of parameter $t$ (see legend). In the inset we show the same plot on a semilog scale in order to illustrate the zero frequency jump—the charge stiffness $D_J^L$.

$$I^L(\omega) = \frac{2}{\beta} \int_0^{\omega+0} \sigma'(\nu) d\nu$$
$$= \frac{1}{L\mathcal{N}} \sum_{n,m}^{n \neq m} |\langle n|J|m \rangle|^2 \theta(\omega+0 - |\phi_m - \phi_n|'),$$
(52)

where $|\eta|' := \min\{|\eta|, 2\pi - |\eta|\}$, and $\theta(x)$ is a Heaviside step function. The integrated conductivity $I^L(\omega)$ is a monotonically increasing function on the frequency interval $\omega \in [0, \pi]$, starting from the charge stiffness

$$I^L(0) = D_J^L,$$
(53)

and satisfying the sum rule on the other end,

$$I^L(\pi) = \frac{1}{L} \langle J^2 \rangle_\rho^L.$$
(54)

Note again that the current variance can be computed [27]:

$$\frac{1}{L} \langle J^2 \rangle_\rho^L = \frac{N(L-N)}{2L(L-1)} = \tfrac{1}{2} \rho(1-\rho) + O\left(\frac{1}{L}\right).$$
(55)

In Fig. 11 we plot the integrated conductivity $I^L(\omega)$ for different values of the kick parameter $t$ (fixed $V=2$) for constant size $L=24$ and density $\rho=1/4$, showing the transition from ergodic $D_J^L \approx 0$ to nonergodic $D_J^L > 0$ dynamics, consistent with results of direct time evolution of Sec. III. In Fig. 12 we analyze the dependence of $I^L(\omega)$ on size $L$ for fixed values of parameters in the nonergodic regime $t=1$, $V=2$, and $\rho=1/4$. Note that for small frequencies $\omega$, $I^L(\omega)$ is roughly constant over the frequency interval $0 \leqslant \omega \leqslant \omega_*^L$, whose width is determined by the Thouless time of a finite system $\mu(L) \sim L$, namely, $\omega_*^L = 2\pi/L$. Note that the expression for stiffness [Eq. (53)] is not completely consistent with the correct definition (10), since the time-limit $\tau \to \infty$ is implicit in Eq. (53) before the TL of increasing $L$ can be considered, whereas the correct order of limits is just the opposite. (This proves another advantage of the numerical study

of direct time evolution discussed in Sec. III over the more common frequency-domain approach presented here.)

An interesting conjecture has been put forward in Ref. [21] (and critically debated in Refs. [43,44]), namely that the half-filled $\rho=1/2$ integrable $t$-$V$ model should exhibit properties of an ideal insulator at all temperatures when $V>t$ (in our notation). The insulating behavior is characterized by $D_J^\infty = I^\infty(0) = 0$ and $(2/\beta)\sigma'(0) = (d/d\omega)I^\infty(0) = 0$, so the time correlation function $C_J(\tau)$ should be an oscillatory function in order to be integrated to zero.

We have found numerical evidence of (at least approximately) insulating behavior even in the nonintegrable half-filled K$t$V model, when $V>t$. In Fig. 13 we demonstrate a double transition from the (for approximately) insulating regime (for example, for $t=0.4$ and $V=1$) to ideally conducting regime (example for $t=V=1$) to the normally conducting regime (example for $t=4.5$ and $V=1$) for a half-filled K$t$V model on $L=16$ sites.
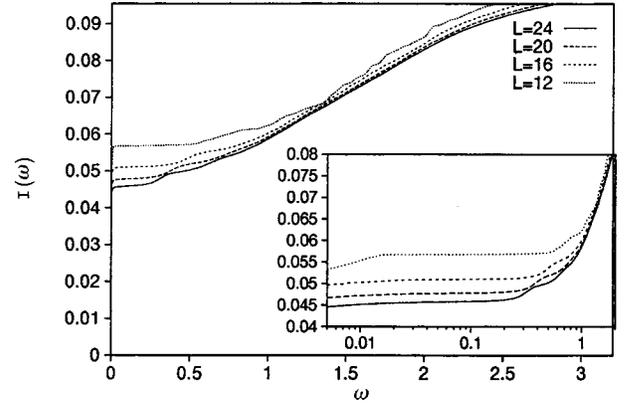
FIG. 12. We show the integrated conductance $I^L(\omega)$ for a quarter filled $\rho=1/4$ cyclic chain at $t=1$ and $V=2$ (in the nonergodic regime) and for different sizes $L=24, 20, 16$, and 12. In the inset we show the same plot on a semilog scale in order to illustrate the convergence of the charge stiffness. Observe that the size of the horizontal plateau at small frequencies shrinks as $\sim 2\pi/L$.
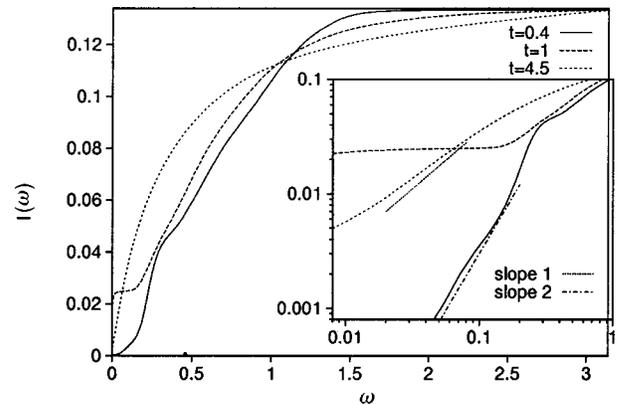


FIG. 13. Integrated conductance $I^L(\omega)$ for a half-filled ($\rho=1/2$) cyclic chain of size $L=16$ is shown for three different values of parameter $t$ (and fixed parameter $V=1$), demonstrating a double transition from insulator (here for $t=0.4$) to ideal conductor (here for $t=1$) to a normal conductor (here for $t=4.5$) as the kick parameter $t$ is increased. In the inset we show the same three curves on a log-log scale.

## V. THIRD METHOD: ALGEBRAIC CONSTRUCTION OF TIME-AVERAGED OBSERVABLES FOR INFINITE SYSTEM

A large amount of numerical evidence has been presented in the previous two sections in support of the conjecture put forward in Sec. I. However, all this evidence is based on computations on many-body systems of finite size $L$, and the TL has been speculated by extrapolation to $1/L=0$. One may still have doubts about whether in a nonintegrable system that is close to an integrable one, quantum ergodicity may squeeze in very slowly for large sizes $L$, beyond the scope of numerical observation. Therefore, as a complementary alternative, one would like to have a method of computation of time correlators, like $D_A$ [Eq. (42)], which would directly operate with infinite systems on infinite lattices $L=\infty$. In this section we elaborate such a method of computation of operator valued time average of an observable $A$ in the Heisenberg representation

$$\bar{A}=\lim_{M\to\infty}\frac{1}{2M+1}\sum_{m=-M}^{M}A(m). \quad (56)$$

The method is specially designed for kicked systems whose propagators can be decomposed into several noncommuting parts [45], and will be implemented to compute time-averaged observables in an infinite $KtV$ model, in particular $\bar{J}$ and $\bar{T}'$, and the corresponding correlators, such as the charge stiffness $D_J$.

### A. Mathematical structures

The first essential mathematical structure used in this section is the Hilbert space of *pseudolocal* quantum observables. Even in the general setting we assume that the evolution propagator preserves the number of particles, $[U,\rho]=0$. So we again fix the density of particles $\rho$ and consider observables $A$ over a Fock (sub)space of quantum states with a given density parameter $\rho$. Such observables preserve the number of particles, $[A,\rho]=0$.

Let us define the *scalar product* of two *extensive* observables $A$ and $B$ as

$$(A|B)=\lim_{L\to\infty}\frac{1}{L}\langle A^{\dagger}B\rangle_{\rho}^{L}=\left\langle\frac{1}{L}A^{\dagger}B\right\rangle_{\rho}. \quad (57)$$

We note that Eq. (57) has all the necessary properties of a scalar (inner) product: it is linear in the right factor, positive, and $(A|B)=(B|A)^{*}$. Note also that averaging over half-filled states is, in the TL, equivalent to the ''grand-canonical'' average, $\langle\cdot\rangle_{\rho=\frac{1}{2}}\equiv\langle\cdot\rangle$.

The observable $A$ is called weakly local or pseudolocal, if $\|A\|^{2}:=(A|A)<\infty$. Pseudolocal observables $A$ constitute a Hilbert space denoted by $\mathfrak{U}$. There is a *linear subspace* $\mathfrak{U}'\subseteq\mathfrak{U}$ of pseudolocal observables $A$, such that $[A,B]=AB-BA$ is pseudolocal for any pseudolocal $B\in\mathfrak{U}$. For any such $A\in\mathfrak{U}'$, the scalar product (57) is an invariant bilinear form with respect to the *adjoint map* $(\text{ad}\,A)B=[A,B]$, namely,

$$((\text{ad}\,A^{\dagger})B|C)=(B|(\text{ad}\,A)C). \quad (58)$$

The second essential mathematical concept is the *unitary* Heisenberg-Floquet map $\hat{U}_{\text{ad}}:\mathfrak{U}\to\mathfrak{U}$, which propagates quantum observables in Heisenberg representation for one period of time, starting at some time $\eta\in[0,1)$:

$$\hat{U}_{\text{ad}}A(\eta+m)=A(\eta+m+1)=U^{\dagger}A(\eta+m)U, \quad (59)$$

$$(\hat{U}_{\text{ad}}A|\hat{U}_{\text{ad}}B)=(A|B). \quad (60)$$

For example, for the $KtV$ model (in spin representation (21) which is, for algebraic convenience, used in this section) we have

$$U\big|_{\eta=1/2}=\exp(-i\tfrac{1}{2}tH_1)\exp(-iV(H_0+\tfrac{1}{2}S_z))\exp(-i\tfrac{1}{2}tH_1), \quad (61)$$

with the potential and kinetic generators

$$H_0=\tfrac{1}{4}\sum_{j=-\infty}^{\infty}\sigma_j^z\sigma_{j+1}^z, \quad (62)$$

$$H_1=\tfrac{1}{4}\sum_{j=-\infty}^{\infty}(\sigma_j^+\sigma_{j+1}^-+\sigma_j^-\sigma_{j+1}^+).$$

Unlike in Sec. III, here we have taken the time steps in the middle between the kicks, $\eta=\tfrac{1}{2}$, in order to fully exploit the time-reversal symmetry of the problem. Note that the time evolution of observables which are diagonal in momentum representation, like $J$ and $T'$, is not affected by the shift $\eta$ of the origin of the stroboscopic map. The Floquet-Heisenberg map can be written explicitly using exponentials of the adjoint maps

$$\hat{U}_{\text{ad}}=\exp[i\tfrac{1}{2}t(\text{ad}\,H_0)]\exp[iV(\text{ad}\,H_1)]\exp[i\tfrac{1}{2}t(\text{ad}\,H_0)]. \quad (63)$$

Since the density $\rho$ (or magnetization $\mathcal{M}=\rho-\tfrac{1}{2}$ in spin-$\tfrac{1}{2}$ formulation) is fixed, the total spin $S_z$ in Eq. (61) generates an irrelevant overall phase which does not influence the evolution of observables.

The time average of the observable (self-adjoint operator) $A$ in Eq. (56) is a solution of the fixed-point equation for the Floquet-Heisenberg map,

$$\hat{U}_{\text{ad}}\bar{A}=\bar{A}. \quad (64)$$

Time averaging in operator space can also be written in terms of an orthogonal projector $\hat{P}_U$ onto the null space of $1-\hat{U}_{\text{ad}}$, namely,

$$\bar{A}=\hat{P}_U A, \quad \hat{P}_U=\lim_{M\to\infty}\frac{1}{2M+1}\sum_{m=-M}^{M}\hat{U}_{\text{ad}}^m. \quad (65)$$

The property

$$\hat{P}_U=\hat{P}_U^2 \quad (66)$$

is easily proved by writing a time-average limit (65) in an equivalent, Gaussian way,

$$\hat{P}_U = \lim_{M\to\infty}\frac{1}{\sqrt{2\pi M}}\sum_{m=-\infty}^{\infty}\exp(-\tfrac{1}{2}(m/M)^2)\hat{U}_{\mathrm{ad}}^m .$$

Without loss of generality we will in the following assume that observable $A$ is traceless $\langle A\rangle=0$, such as $J$ and $T'$. Note that the generalized stiffness (42) can be written simply as

$$D_A=(A|\bar{A}). \qquad (67)$$

### B. Time average from variational principle in operator space

The scaled (or normalized) time average of a self-adjoint operator $A=A^{\dagger}$, $X=\bar{A}/\|\bar{A}\|$, can be obtained from a *variational principle in operator space*, that is, as an extremum (*maximum*) of an action $s(X)$,

$$\frac{\delta}{\delta X}s(X)=0,$$

$$s(X)=\tfrac{1}{2}(X|A)(A|X)=\tfrac{1}{2}|(X|A)|^2, \qquad (68)$$

with constraints

$$\|(1-\hat{U}_{\mathrm{ad}})X\|^2=(X|(1-\hat{U}_{\mathrm{ad}}^{-1})(1-\hat{U}_{\mathrm{ad}})|X)=0, \quad (69)$$

$$(X|X)=\mathrm{const}<\infty, \qquad (70)$$

that is, Eqs. (68)–(70) imply $X=\alpha\bar{A}$, where $\alpha=\|\bar{A}\|^{-1}$ if $X$ is normalized as $(X|X)=1$. Since the constraint (69) is homogeneous, the corresponding Lagrange multiplier is diverging. Hence, we suggest to write the constrained variational problem [Eqs. (68)–(70)] in the compact form

$$\lim_{\epsilon\to 0}\frac{\delta}{\delta X}s_{\epsilon}(X)=0 \;\Rightarrow\; X=\alpha\bar{A}, \quad \alpha\in\mathbb{C},$$
$$(71)$$
$$s_{\epsilon}(X)=\tfrac{1}{2}|(X|A)|^2-\tfrac{1}{2}\lambda\|\epsilon^{-1}(1-e^{-\epsilon}\hat{U}_{\mathrm{ad}})X\|^2$$

where $\lambda$ is another Lagrange multiplier associated with the second constraint (70). Indeed, for small $\epsilon$ one may write

$$s_{\epsilon}(X)=\tfrac{1}{2}|(X|A)|^2-\tfrac{1}{2}\lambda(X|X)$$
$$-\tfrac{1}{2}\lambda(\epsilon^{-2}-\epsilon^{-1})\|(1-\hat{U}_{\mathrm{ad}})X\|^2+O(\epsilon),$$

so homogeneous constraint (69) follows automatically as $\epsilon\to 0$ in order to make the action $s_{\epsilon}(X)$ regular (and maximal) at $\epsilon=0$. Let us now show that the above variational problem (71) has the correct solution (56). We differentiate action (71),

$$\frac{\delta}{\delta X}s_{\epsilon}(X_{\epsilon})=(A|X_{\epsilon})A-\frac{\lambda}{\epsilon^2}(1-e^{-\epsilon}\hat{U}_{\mathrm{ad}}^{-1})(1-e^{-\epsilon}\hat{U}_{\mathrm{ad}})X_{\epsilon}$$

$$=0,$$

and write $a=(A|X)$. This equation can be solved explicitly for $X_{\epsilon}$:

$$X_{\epsilon}=\frac{a\epsilon^2}{\lambda}(1-e^{-\epsilon}\hat{U}_{\mathrm{ad}})^{-1}(1-e^{-\epsilon}\hat{U}_{\mathrm{ad}}^{-1})^{-1}A$$

$$=\frac{a\epsilon^2}{\lambda}\sum_{n=0}^{\infty}\sum_{m=0}^{\infty}e^{-(n+m)\epsilon}\hat{U}_{\mathrm{ad}}^{n-m}A$$

$$=\frac{a\epsilon^2}{\lambda}\sum_{p=-\infty}^{\infty}A(p)\sum_{q=|p/2|}^{\infty}e^{-q\epsilon}$$

$$=\frac{a\epsilon^2}{\lambda(1-e^{-\epsilon})}\sum_{p=-\infty}^{\infty}A(p)e^{-(\epsilon/2)|p|}. \qquad (72)$$

In the limit $\epsilon\to 0$, the last expression (72) is proportional to the time average

$$X=\lim_{\epsilon\to 0}X_{\epsilon}=\frac{4a}{\lambda}\bar{A}. \qquad (73)$$

Evaluation

$$a=(A|X)=a\frac{4D_A}{\lambda}$$

fixes the value of the Lagrange multiplier

$$\lambda=4D_A . \qquad (74)$$

The unitarity [Eq. (60)] and invariance [Eq. (64)] have the following very important consequence:

$$(\bar{A}|\bar{A})=(A|\bar{A})=(\bar{A}|A). \qquad (75)$$

Assuming that $X$ is nonvanishing so that $(X|X)>0$, and that $X$ and $\bar{A}$ are *proportional*, one can write

$$\bar{A}=\frac{(X|\bar{A})}{(X|X)}X=\frac{(X|A)}{(X|X)}X. \qquad (76)$$

Taking the scalar product of the last equation with $A$, one obtains a very useful expression for the stiffness:

$$D_A=\frac{|(A|X)|^2}{(X|X)}. \qquad (77)$$

### C. Numerical application

However, the maximization of functionals (68) and (71) in the huge infinitely dimensional operator space $\mathfrak{U}$ is not convenient for practical calculation. Instead, we suggest estimating the time-averaged observable $\bar{A}$ by solving the variational problem (71) in a finite-dimensional subspace $\mathfrak{M}(A)\subset\mathfrak{U}$ (the Galerkin-like approach in operator space). In fact, we devise a special sequence of truncated ''minimal invariant'' operator spaces $\ldots\mathfrak{M}_p(A)\subset\mathfrak{M}_{p+1}(A)\ldots\subset\mathfrak{U}$, which in the limit $p\to\infty$ (after closure), contain the time average $\bar{A}$. Thus the solutions $X_p$ of the variational problems (71) on spaces $\mathfrak{M}_p$ should converge to the proper scaled time average $X$ of observable $A$.

Let $\mathfrak{s}=\{\alpha H_0+\beta H_1;\alpha,\beta\in\mathbb{C}\}$ be a two-dimensional linear vector space spanned by the two generators of motion,

$H_\alpha, \alpha = 0$ and 1 [Eq. (62)]. Let us define the *minimal invariant operator space containing A*, as the closure of linear combinations of all products of adjoint generators ad $H_\alpha, \alpha = 0$ and 1 on $A$:

$$\mathfrak{M}(A) = \overline{\cup_{n=0}^{\infty} (\text{ad } \mathfrak{s})^n A}. \tag{78}$$

$\mathfrak{M}(A)$ is indeed the minimal (though infinitely dimensional in general) operator space containing $A$ with the invariance property

$$(\text{ad } H_\alpha)\mathfrak{M}(A) = \mathfrak{M}(A), \quad \alpha = 0,1,$$
$$\hat{U}_{\text{ad}} \mathfrak{M}(A) = \mathfrak{M}(A), \quad \forall t, V. \tag{79}$$

From the construction of the time average (65), it is obvious that $\bar{A} \in \mathfrak{M}(A)$. We now construct the countable basis of the space $\mathfrak{M}(A)$ ordered by the order of locality as follows: We assign an observable $\tilde{H}_{q,c}$ to an *ordered pair* of integers $(q,c)$, *order* $q$, and *code* $c$, $0 \le c < 2^{q-1}$ with $q-1$ binary digits $c_n$, $c = \Sigma_{n=1}^{q-1} c_n 2^{n-1}$, namely,

$$\tilde{H}_{q,c} = (\text{ad } H_{c_{q-1}})(\text{ad } H_{c_{q-2}}) \cdots (\text{ad } H_{c_1}) A. \tag{80}$$

Since not all observables $\tilde{H}_{q,c}$ up to a given maximal order $p, q \le p$, are linearly independent we perform Gram-Schmit orthogonalization with respect to the scalar product (57)

$$G_{q,c} = \begin{cases} \tilde{G}_{q,c}/\sqrt{(\tilde{G}_{q,c}|\tilde{G}_{q,c})}, & \tilde{G}_{q,c} \ne 0 \\ 0, & \tilde{G}_{q,c} = 0, \end{cases}$$
$$\tilde{G}_{q,c} = \tilde{H}_{q,c} - \sum_{(r,b)}^{(r,b)<(q,c)} G_{r,b}(G_{r,b}|\tilde{H}_{q,c}). \tag{81}$$

The nonzero observables $G_{q,c}$ form the orthonormal basis of $\mathfrak{M}(A)$. Note that observables $G_{q,c}$ are strictly local operators of order $q$: in the case of spin representation of K$t$V model, they are represented as expansions

$$G_{q,c} = \sum_{s_0, s_1, \ldots s_q} g_{q,c}^{s_0 s_1, \ldots, s_q} Z_{s_0 s_1, \ldots, s_q} \tag{82}$$

in terms of spatially homogeneous finite products of field operators:

$$Z_{s_0 s_1, \ldots, s_q} = \sum_{j=-\infty}^{\infty} \sigma_j^{s_0} \sigma_{j+1}^{s_1} \cdots \sigma_{j+q}^{s_q},$$

where $s_k \in \{0, +, -, z\}$ and $\sigma_j^0 = 1$. The (average) number of nonzero terms in expansions (82) was found to grow exponentially at approximately the same rate for both observables under study, for either $A = J$ or $A = T'$, namely, as

$$\#\{g_{q,c}^{s_0 s_1, \ldots, s_q} \ne 0\} \approx 0.5 \times 2.55^q,$$

which may be further reduced by a factor 2, or even by a factor 4 if $\rho = \frac{1}{2}$, using the symmetries $\hat{\mathcal{P}}$ [Eq. (26)], and $\hat{\mathcal{R}}$ [Eq. (27)] (the latter may be used only if $\rho = \frac{1}{2}$). Note that the entire linear space $\mathfrak{M}(A)$ has the same symmetry properties as observable $A$, for example, the space $\mathfrak{M}(J)$ and $\mathfrak{M}(T')$

TABLE II. Dimensions of the truncated minimal invariant spaces and of the null spaces of truncated adjoint maps for different orders of truncation $p$.

| $p$ | $d_p(J)$ | $d_{p,0}(J)$ | $d_{p,1}(J)$ | $d_p(T')$ | $d_{p,0}(T')$ | $d_{p,1}(T')$ |
|---|---|---|---|---|---|---|
| 1 | 1 | 1 | 1 | 1 | 0 | 1 |
| 2 | 2 | 0 | 2 | 2 | 0 | 1 |
| 3 | 4 | 2 | 2 | 4 | 1 | 2 |
| 4 | 7 | 3 | 3 | 6 | 2 | 1 |
| 5 | 12 | 6 | 4 | 10 | 4 | 5 |
| 6 | 21 | 9 | 7 | 15 | 5 | 2 |
| 7 | 38 | 16 | 12 | 25 | 9 | 10 |
| 8 | 69 | 27 | 21 | 40 | 12 | 7 |
| 9 | 126 | 48 | 38 | 66 | 22 | 21 |
| 10 | 230 | 84 | 68 | 107 | 33 | 22 |
| 11 | 419 | 153 | 123 | 178 | 60 | 51 |
| 12 | 763 | 273 | 223 | 293 | 91 | 66 |
| 13 | 1393 | 493 | 409 | 494 | 162 | 137 |
| 14 | - | - | - | 831 | 257 | 202 |

belong to a negative and positive parity symmetry class, respectively, with respect to parity operation (26).

Let us now define a sequence of *truncated minimal invariant operator spaces* containing $A$,

$$\mathfrak{M}_p(A) = \cup_{n=0}^{p-1}(\text{ad } \mathfrak{s})^n A, \quad p = 1, 2 \ldots, \tag{83}$$

with dimensions $d_p(A) := \dim \mathfrak{M}_p(A)$. Linear space $\mathfrak{M}_p(A)$ contains operators derived from $A$ by composition of generators ad $H_\alpha$ up to *order p*. Due to binary code construction (80) we have a strict upper bound on the growth of dimensions of the truncated spaces $\mathfrak{M}_p(A)$,

$$d_p(A) \le 2^{p-1}; \tag{84}$$

however, actual dimensions may grow considerably more slowly (due to systematic linear dependences among $\tilde{H}_{p,b}$); that is, for $A = J$ and $A = T'$, by computer algebra up to $p = 14$th order (see Table II), we find empirically

$$d_p(J) \approx 1.825^{p-1}, \quad d_p(T') \approx 1.68^{p-1}. \tag{85}$$

Let $\mathbf{H}_{p,\alpha}$, $\alpha = 0$ and 1, denote real and symmetric (Hermitian in general) matrices of linear maps and $H_\alpha$ on $\mathfrak{M}_p(A)$ with images orthogonally projected back to $\mathfrak{M}_p(A)$. It follows from the construction that they have (generally) a block-banded structure, where the blocks correspond to observables with a fixed order $q$:

$$(G_{q,c}|\text{ad } H_\alpha|G_{q',c'}) = 0, \quad \text{if } |q - q'| \ne 1. \tag{86}$$

The truncated adjoint maps $\mathbf{H}_{p,\alpha}$ have nontrivial null spaces

$$\mathfrak{N}_{p,\alpha}(A) = \{B \in \mathfrak{M}_p(A); [H_\alpha, B] \in \mathfrak{M}_{p+1}(A) - \mathfrak{M}_p(A)\}, \tag{87}$$

with dimensions $d_{p,\alpha}(A) := \dim \mathfrak{N}_{p,\alpha}(A)$ which increase approximately with the same exponent as $d_p(A)$ [Eq. (85)] (see Table II).

By means of truncated adjoint maps $\mathbf{H}_{p,\alpha}$ we construct an approximate Floquet-Heiseberg matrix $\mathbf{U}_p$, which is a $d_p(A)$-dimensional *unitary* matrix over the truncated space $\mathfrak{M}_p(A)$:

$$\mathbf{U}_p = \exp(i\tfrac{1}{2}t\mathbf{H}_{p,1})\exp(iV\mathbf{H}_{p,0})\exp(i\tfrac{1}{2}t\mathbf{H}_{p,1}). \quad (88)$$

Now we are ready to solve the variational problem [Eqs. (68)–(71)] in the truncated space $\mathfrak{M}_p(A)$. We note an important ''experimental'' observation (whose theoretical understanding is stil lacking) namely, that the matrix $\mathbf{1}-\mathbf{U}_p$ possesses a high-dimensional null space

$$\mathfrak{N}_p^U(A)=\{B\in\mathfrak{M}_p(A);\mathbf{U}_pB=B\},$$

whose dimension $d_p^U(A):=\dim\mathfrak{N}_p^U(A)$ is, for odd $p$, independent of parameters $t$ and $V$ and equal to the dimension of the null space of $\mathbf{H}_{p,1}$:

$$d_{2l-1}^U(A)=d_{2l-1,1}(A). \quad (89)$$

Note also that for odd order of truncation $p=2l-1$, the elements of null space $B\in\mathfrak{N}_p^U(A)$ are spanned by combinations of *even* powers of generators only, i.e., $(B|G_{2l,c})\equiv0$, which is due to time-symmetric construction ($\eta=\tfrac{1}{2}$) of the evolution operator $\hat{U}_{\mathrm{ad}}$ (63).

The scalar products (57) for different values of the density $\rho$ are nondegenerate with respect to each other, and therefore the dimensions of various linear (sub)spaces, $d_p(A),d_{p,\alpha}(A),d_p^U(A)$, (see Table II) *do not depend* on the density parameter $\rho$.

The constraint (69) is now equivalent to restricting the variation (68) to the subspace $\mathfrak{N}_p^U(A)$. Hence the ''truncated'' scaled time-averaged observable $X_p$ is a maximum of the quadratic form $(X_p|A)(A|X_p)$ on $\mathfrak{N}^U(A)$ with a normalization constraint $(X_p|X_p)=1$. In other words, if $F_n$, $n=1,\dots,d:=d_p^U(A)$ is an orthonormal basis of the null-space $\mathfrak{N}_p^U(A)$, and, if $(x_1,\dots,x_d)$ is a normalized eigenvector of the (positive definite) $d\times d$ matrix eigenvalue problem,

$$\sum_n (F_m|A)(A|F_n)x_n=fx_m,$$

with the *maximal* eigenvalue $f$, then

$$X_p=\sum_n F_n x_n \quad (90)$$

is a solution of the variational problem [Eqs. (68)–(71)] in the truncated space $\mathfrak{M}_p(A)$. In the limit $p\to\infty$ we expect to recover an exact time average

$$\lim_{p\to\infty} X_p=X=\|A\|^{-1}\bar{A}. \quad (91)$$

However, if the system is ergodic, the time average should be zero $\bar{A}=0$ (note that $\langle A\rangle=0$), so the (normalizable) limit (91) should not exist. In order to inspect the convergence of
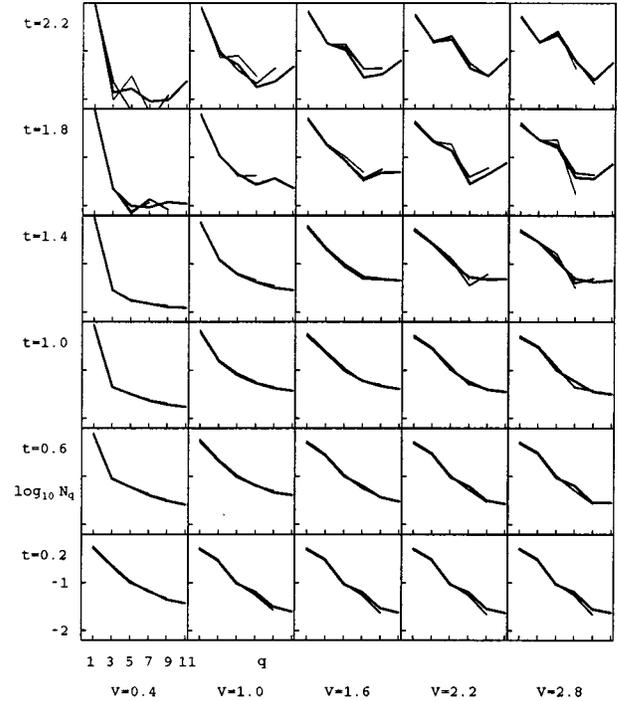


FIG. 14. The logarithm of the relative norm $N_q(X)$ of the normalized time-averaged current $X=\bar{J}/\|J\|$ in a quarter-filled ($\rho=1/4$) infinite K$t$V model is plotted against (odd) order $q=2l-1$, for a square mesh of parameters $t$ and $V$. The three different curves on each graph, thick, medium, and thin, refer to three different orders of truncation of operator spaces, $p=11$, 9, and 7, respectively.

$X_p$ in the Hilbert space of observables $\mathfrak{U}$, we define a *relative norm* $N_q(X)$ with respect to order $q$:

$$N_q(X)=\sum_c |(X|G_{q,c})|^2. \quad (92)$$

Since

$$\|X\|^2=\sum_{q=0}^\infty N_q(X), \quad (93)$$

the inspection of the convergence of the sum on the right-hand side of Eq. (93) would give us an indication of the convergence of $X_p$ [Eq. (91)] and thus of the nonergodicity of the problem. As a second criterion of convergence of $X$, we study the *stability* of $X_p$, or of the relative norms $N_q(X_p),q\leqslant p$, with respect to the variation of the truncation order $p$.

In Figs. 14 and 15 we show the relative norms $N_q(X_p)$ of the normalized time average of the current $J$ (Fig. 14) and kinetic energy $T'$ (Fig. 15) for several different orders of truncation $p$ (up to $p=11$ for $J$ and up to $p=13$ for $T'$). We note that, for both observables, $X_p$ is quite stable against variation of $p$, for $t\leqslant1.4$; also, in the same parameter range, the coefficients $N_q(X_p)$ seem to be summable. The stiffness $D_A$ [Eq. (77)] may be rewritten in terms of relative norms as
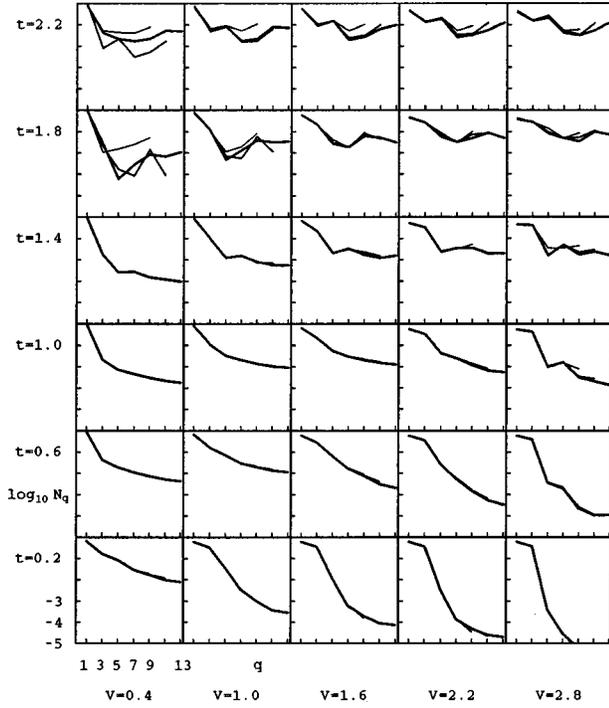
FIG. 15. Same as in Fig. 14 for the normalized time-averaged kinetic energy $X = \bar{T}'/\|T'\|$, but for larger truncation orders, $p = 13$ (thick curves), $p = 11$ (medium curves), and $p = 7$ (thin curves).

$$D_A = (A|A) \frac{N_1(X)}{\sum_{q=1}^{\infty} N_q(X)}. \qquad (94)$$

In this regime where $X$ is convergent in $\mathfrak{U}$, $N_q(X_p)$ are good approximations of $N_q(X)$ for $q \lesssim p$ [apart from a constant renormalization prefactor which cancels out from expressions like Eq. (94)], and we may write a good estimate for the upper bound on the stiffness

$$D_A^p = |(A|X_p)|^2 \approx (A|A) \frac{N_1(X)}{\sum_{q=1}^{p} N_q(X)}$$

$$> (A|A) \frac{N_1(X)}{\sum_{q=1}^{\infty} N_q(X)} = D_A^{\infty}. \qquad (95)$$

However, we would like to have accurate approximations of the stiffness $D_A^{\infty}$ itself rather than just the upper bounds, so we extrapolate the relative norms $N_q(X) \approx N_q(X_p)$ to orders higher than the order of truncation, $q > p$, in an expression for the stiffness [Eq. (94)] by fitting the tail of $N_{q=2l+1}(X_p)$ at three points: $q = p-4, p-2$, and $p$ [note that $N_{q=2l}(X_p) = 0$] with exponential ansatz $N_{q=2l+1}(X_p) \propto \exp(-sq)$. Since the actual rate of convergence of $N_q(X) \to 0$, as $q \to \infty$ seems to be slower than exponential (see Figs. 14 and 15), the stiffness extrapolated in this way [Eq. (94)], $D_A^e$, is
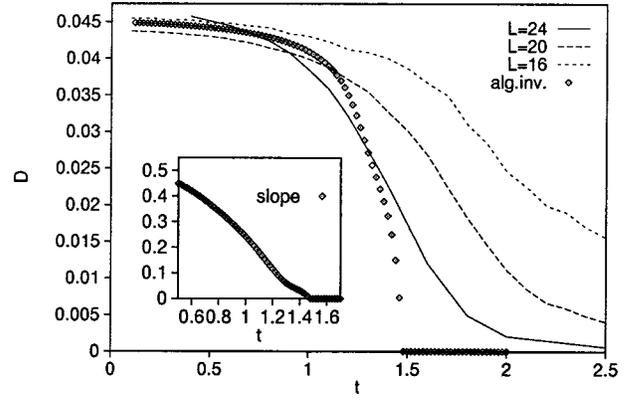


FIG. 16. Charge stiffness $D_J$ vs kick parameter $t$ and constant parameter $V = 2$ for a quarter-filled chain $\rho = 1/4$. Different curves refer to different system sizes $L = 24$, 20, and 16, while points represent the infinite-size stiffness [Eq. (77)] based on an extrapolated algebraic time-averaged current invariant of motion. The truncation order is $p = 11$. In the inset we show the logarithmic slope $s$ of the falloff of the relative norms $N_q(\bar{J}) \propto \exp(-sq)$ at $q \approx p$.

expected to be still slightly overestimated. In Fig. 16 we show the dependence of the extrapolated charge stiffness $D_J^e$ on the parameter $t$ (and for fixed $V = 2$) through the critical range $t \sim t_c \approx 1.45$, and compare it with the charge stiffness as computed from direct diagonalization of the finite K$tV$ chains of sizes $L = 24$, 20, and 16. When approaching the critical point $t_c$, the fitted slope $s$ linearly decreases to zero. For larger values of parameters, $t > t_c(V)$, $X_p$ is not stable against variation of $p$ and the partial sums of relative norms $N_q(X)$ are not converging. Therefore, $\bar{A} = 0$ and $D_A^{\infty} = 0$, and the system is quantum ergodic. In Fig. 17 we plot a full $(t, V)$ phase diagram of the (extrapolated) charge stiffness $D_J^e$. It is clear that this last method, since in operates with an infinite system, gives the most reliable results on the critical regions of transition between dynamical phases. However, no other dynamical information on correlation functions is obtained other than their time averages, so within the present method
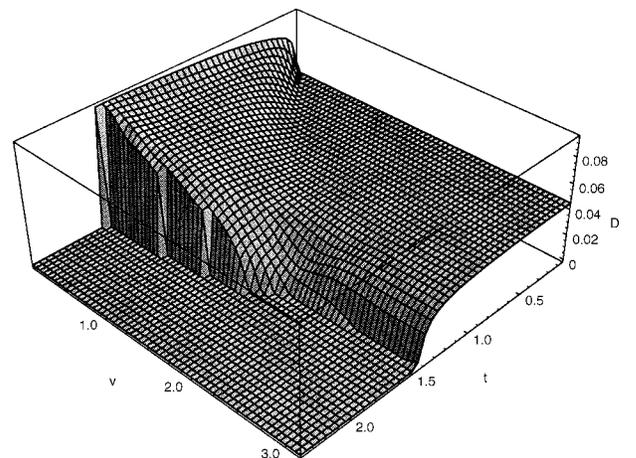


FIG. 17. $(t, V)$ phase diagram of the charge stiffness $D_J$ for a quarter-filled ($\rho = 1/4$) infinite K$tV$ model, as deduced from an *extrapolated* time-averaged current $\bar{J}$.

we cannot make any claims on the stronger ergodic property of quantum mixing.

Although the dynamical behavior of observables may in principle depend on the symmetry class of observables with respect to, say, parity operation (26), we have found very similar ergodic, nonergodic, and critical regions, for the two examples of opposite parity observables, $J$ and $T'$, that have been studied. However, we should note that dynamical behavior may also depend on the other (continuous) conserved quantities, such as the density $\rho$. Our results for other values of density $\rho$ indicate that the transition region between ergodic and nonergodic dynamics moves to slightly smaller values of parameter $t$ as $\rho$ approaches $1/2$. Due to particle-hole transformation [Eq. (27)], the dynamics for $\rho=\rho'$ is equivalent to the dynamics for $\rho=1-\rho'$.

We should note that in a recent paper [46] a very similar algebraic approach was used in order to compute numerically the pseudolocal quantum invariants of motion. In the regime of nonergodic dynamics one or two converged pseudolocal invariants of motion were found, whereas in the regime of ergodic dynamics, consistently, no nontrivial invariants of motion were found. Then by using a formula [Eq. (11)] of Mazur [24] and Suzuki [25], the time-averaged correlation of kinetic energy $D_T$ has been computed by means of an expansion in terms of pseudolocal invariants, giving results which are in good agreement with the results of direct calculations on finite systems. We believe that our variational approach in the space of observables presented here is (in general, possibly nonintegrable case) an improvement of the Mazur-Suzuki approach [24,25] to the calculation or estimation of time-averaged correlators. Within Mazur formula (11) one is typically able to write only the inequality (the lower bound on the stiffness), since the set of *known local* invariants of motion may be *incomplete*.

## VI. CONCLUSIONS AND DISCUSSION

In this paper we have presented three complementary (mainly numerical and computer-algebraic) approaches to the dynamics of nonintegrable quantum many-body systems in the thermodynamic limit (TL), demonstrated and studied in a kicked $(t,V)$ model of spinless fermions. We have been primarily interested in the structural stability of nonergodic quantum motion and the transition from nonergodic and non-mixing to ergodic/mixing dynamics in the TL.

The first approach that we used is a direct time evolution of a finite quantum system (which may be in the present model performed very efficiently by means of the so-called fermionic fast Fourier transformation) and computation of time correlation functions of generic quantum observables. The size $L$ of the system is systematically increased, and the TL is speculated based on extrapolation to $1/L=0$. For sufficiently large values of kick parameters, we have found quantum mixing and *exponential* decay of time correlation functions, while for smaller, intermediate values ($\sim 1$) of kick parameters, we have found nonmixing quantum motion characterized by saturating, nonvanishing time correlation functions.

Our second approach is a direct diagonalization of the stationary quantum problem of finite size, and a calculation of dynamical properties, such as charge stiffness, conductivity, etc., in the frequency domain. Also, traditional quantum signatures of chaos, such as level statistics, have been inspected and shown to correspond with the dynamical behavior. This approach is less computationally efficient in the case of the present model than the first one.

In the third approach, which is fully complementary to the other two, we propose an algebraic method for computation of time-averaged observables of an infinite system. Thus we can make very precise statements on the quantum ergodicity of an infinite system, which are in complete agreement with the extrapolated results of calculations on finite systems.

The above results are claimed to be the evidence for the validity of the conjecture in Sec. I, namely, that the generic quantum many-body system in the TL may not be quantum ergodic (or mixing) if it is sufficiently close to an integrable system in parameter space. Recent numerical results on transport in the extended (nonintegrable) Hubbard model [43] are compatible with the above conjecture. The transition between nonergodic and ergodic dynamics when the external parameters are increased has the properties of a (dynamical) phase transition and should be further studied theoretically. The first such attempt to do this was undertaken in Ref. [15], where a discretized nonintegrable quantum field model (in the continuum limit) was mapped on a quantum chaotic model of a single particle on a 2D torus (in the quasiclassical limit), and the transition from nonergodic and nonmixing dynamics to ergodic and mixing dynamics of the quantum field model has been identified with the stochastic transition from regular to chaotic motion.

We have also given a clear evidence on the nontrivial existence of *mixing quantum motion* in the K$tV$ model in the TL with *exponentially* decreasing time correlation functions, provided the external (kick) parameters are large enough (above the critical values). Such quantum mixing behavior may be a source of truly *chaotic* and *macroscopically irreversible* quantum motion of many-body systems [47]. Note that macroscopic irreversibility as a consequence of *nondissipative* but strongly nonintegrable quantum many-body dynamics has been recently observed experimentally [48].

One might doubtfully argue that our quite surprising finding on structurally stable nonergodic quantum motion in the TL (formulated as the conjecture in Sec.I) may be just another peculiarity of physics in one-dimension, and as such should not be expected to hold in interacting quantum systems in more than one spatial dimension. Being aware of this fear we have straightforwardly extended our K$tV$ model [Eqs. (12) and (13)] to a rectangular periodic $L_1 \times L_2$ lattice in two spatial dimensions, with isotropic hopping in two orthogonal directions and $\delta$-kicked isotropic nearest neighbor interaction. An efficient direct time evolution of the 2D K$tV$ model has been implemented analogously along the lines described in Sec. III, and its time correlation functions have been computed accordingly, though due to the greater computational complexity only for relatively small lattices of sizes up to $6 \times 5$. We should stress that we were again able to identify quite clearly the two regimes of quantum motion which have been roughly stable against the variation of the

lattice size, namely, (i) a quantum mixing regime for sufficiently large $t$ and $V$, and more importantly, (ii) a quantum nonergodic and nonmixing regime for $|t| \sim |V| \sim \frac{1}{2}$ (or smaller), although the system is not known to be analytically integrable in the limit $t \to 0, V \to 0$. This result (whose details will be published elsewhere) is a small piece of numerical evidence for the validity of the conjecture in two spatial dimensions.

[1] I. Kornfeld, S. Fomin, and Ya. Sinai, *Ergodic Theory* (Springer, New York, 1982).

[2] V. I. Arnold and A. Avez, *Ergodic Problems of Classical Mechanics* (Benjamin, New York, 1968).

[3] M. Henon, in *Chaotic behaviour of Deterministic Systems*, edited by G. Iooss, R.H.G. Helleman, and R. Stora, Les Houches 1981 Proceedings (North-Holland, Amsterdam, 1983).

[4] G. Gallavotti and E.G.D. Cohen, Phys. Rev. Lett. **74**, 2694 (1995); J. Stat. Phys. **80**, 931 (1995).

[5] E. Fermi, J. Pasta, S. Ulam, and M. Tsingou, Los Alamos Report No. LA-1940, 1955 (unpublished); E. Fermi, *Collected Papers* (University of Chicago Press, Chicago, 1965), Vol. 2, p. 978.

[6] S. Lepri, R. Livi, and A. Politi, Phys. Rev. Lett. **78**, 1896 (1997); Physica D **119**, 140 (1998).

[7] D.L. Shepelyansky, Nonlinearity **10**, 1331 (1997).

[8] B.V. Chirikov and F.M. Izrailev, Dokl. Akad. Nauk SSSR **166**, 57 (1967) [Sov. Phys. Dokl. **11**, 30 (1966)]; B.V. Chirikov, F.M. Izrailev, and V.A. Tayursky, Comput. Phys. Commun. **5**, 11 (1973).

[9] We would like to demonstrate statistical laws with minimal external randomness. Hence we think of an isolated system left to evolve with no contact with thermal reservoirs of any kind, since we would like to inspect how nonlinear interaction alone can control the ergodic properties of dynamics.

[10] For example, one may generally take $f(e^{-i\varphi}) = \sum_{n=-\infty}^{\infty} f_n e^{-in\varphi}$ to be a a strong limit of trigonometric polynomials, $\{f_n\} \in \ell_2$, such as are the projection operators $E_\varphi$ according to the spectral theorem for unitary operators [11].

[11] N. Dunford and J.T. Schwartz, *Linear Operators, Part II: Spectral Theory* (Interscience, New York, 1963).

[12] M.L. Mehta, *Random Matrices* (Academic Press, London, 1991).

[13] M. Gutzwiller, *Chaos in Classical and Quantum Mechanics*, (Springer-Verlag, New York, 1990), F. Haake, *Quantum Signatures of Chaos* (Springer-Verlag, Berlin, 1991); *Quantum Chaos: Between Order and Disorder*, edited by G. Casati and B. Chirikov (Cambridge University Press, Cambridge, 1995).

[14] *Chaos and Quantum Physics*, edited by M.-J. Giannoni, A. Voros, and J. Zinn-Justin, Les Houches 1989 Proceedings (North-Holland, Amsterdam, 1991).

[15] T. Prosen, Phys. Rev. E **60**, 1658 (1999).

[16] S. Graffi and A. Martinez, J. Math. Phys. **37**, 5111 (1996).

[17] M. Lenci, J. Math. Phys. **37**, 5137 (1996).

[18] G. Jona-Lasinio and C. Presilla, Phys. Rev. Lett. **77**, 4322 (1996); P. Castiglione, G. Jona-Lasinuo, and C. Presilla, J. Phys. A **29**, 6169 (1996).

[19] V.V. Flambaum, F. Izrailev, and G. Casati, Phys. Rev. E **54**,

2136 (1996); V.V. Flambaum, A.A. Gribakina, G.F. Gribakin, and I.V. Ponomarev, e-print, cond-mat/9711213.

[20] G. Montambaux, D. Poilblanc, J. Bellissard, and C. Sire, Phys. Rev. Lett. **70**, 497 (1993); D. Poilblanc, T. Ziman, J. Bellissard, F. Mila, and G. Montambaux, Europhys. Lett. **22**, 537 (1993); T.C. Hsu and J.C. Angles d'Auriac, Phys. Rev. B **47**, 14 291 (1993).

[21] X. Zotos and P. Prelovšek, Phys. Rev. B **53**, 983 (1996); H. Castella, X. Zotos, and P. Prelovšek, Phys. Rev. Lett. **74**, 972 (1995).

[22] X. Zotos, F. Naef, and P. Prelovšek, Phys. Rev. B **55**, 11 029 (1997).

[23] R. Kubo, J. Phys. Soc. Jpn. **12**, 570 (1957).

[24] P. Mazur, Physica (Amsterdam) **43**, 533 (1969).

[25] M. Suzuki, Physica (Amsterdam) **51**, 277 (1971).

[26] Precise conditions on the ''generic'' class of interactions are yet to be determined; here we show the conjecture for a particular specific example and quote few other results (Sec. VI). However, we should stress that we have in mind only purely *deterministic systems* and nonrandom interactions, so Hamiltonians $H_\lambda$ of infinite systems are supposed to be prescribed using a *finite* amount of information.

[27] T. Prosen, Phys. Rev. Lett. **80**, 1808 (1998).

[28] V.E. Korepin, N. M. Bogoliubov, and A.G. Izergin, *Quantum Inverse Scattering Method and Correlation Functions* (Cambridge University Press, Cambridge, 1993).

[29] P. Jordan and E. Wigner, Z. Phys. **47**, 631 (1928).

[30] G. Casati, B.V. Chirikov, F. M. Izrailev, and J. Ford, in *Stochastic Behavior in Classical and Quantum Hamiltonian Systems*, edited by G. Casati and J. Ford, Lecture Notes in Physics Vol. 93 (Springer, New York, 1979).

[31] R. Artuso, G. Casati, F. Borgonovi, L. Rebuzzini, and I. Guarneri, Int. J. Mod. Phys. B **8**, 207 (1994).

[32] W. H. Press, S. A. Teukolsky, W. T. Vetterling, and B. P. Flannery, *Numerical Recipes*, 2nd ed. (Cambridge University Press, Cambridge, 1992).

[33] S. Winograd, *Arithmetic Complexity of Computations* (SIAM, Philadelphia, 1980).

[34] O. Bohigas, M.-J. Giannoni, and C. Schmit, Phys. Rev. Lett. **52**, 1 (1984).

[35] O. Bohigas, in *Chaos and Quantum Physics* (Ref. [14]).

[36] A. V. Andreev, O. Agam, B.D. Simons, and B.L. Altshuler, Phys. Rev. Lett. **76**, 3947 (1996).

[37] M. V. Berry and M. Tabor, Proc. R. Soc. London, Ser. A **156**, 375 (1977).

[38] M.V. Berry and M. Robnik, J. Phys. A **17**, 2413 (1984).

[39] T. Prosen and M. Robnik, J. Phys. A **27**, 8059 (1994).

[40] E.B. Bogomolny, U. Gerland, and C. Schmit, Phys. Rev. E **59**, R1315 (1999).

[41] D. Braun, G. Montambaux, and M. Pascaud, e-print cond-mat/9712256.

[42] M.V. Berry, Proc. R. Soc. London, Ser. A **400**, 229 (1985).

[43] S. Kirchner, H. G. Evertz, and W. Hanke, e-print, cond-mat/9804148.

[44] S. Fujimoto and N. Kawakami, J. Phys. A **31**, 465 (1998); N.M.R. Peres, P.D. Sacramento, D.K. Campbell, and J.M.P. Carmelo, e-print, cond-mat/9804169.

[45] A simpler and perhaps more powerful version of the method for autonomous Hamiltonian systems, which may be used also to give rigorous upper bounds on charge or spin stiffness, etc., will be presented elsewhere.

[46] T. Prosen, J. Phys. A **31**, L645 (1998).

[47] T. Prosen, G. Usaj, and H. M. Pastawski (unpublished).

[48] G. Usaj, H.M. Pastawski, and P.R. Levstein, e-print, cond-mat/9803047.